Marine heatwave and keystone predator loss drive broad-scale decline and hinder recovery of a rocky intertidal kelp

Running title: Heatwave and disease drive kelp decline

Francis D. Gerraty[1*] (*ORCID*: 0000-0001-9989-4953), Karah N. Cox-Ammann[1](ORCID: 0000-0002-6200-1944), Melissa A. Douglas[1], Maya George[1], David P. Lohse[1], C. Melissa Miner[1] (*ORCID*: 0000-0002-4032-3846), Peter T. Raimondi[1] (*ORCID*: 0000-0001-5235-1441)

[1]University of California—Santa Cruz, Department of Ecology and Evolutionary Biology, Santa Cruz, California, United States.
*corresponding author: Phone: (415)686-3300. Email: fgerraty@ucsc.edu

Abstract:

Human activities are increasingly driving the co-occurrence of multiple ecological stressors, resulting in interactive and cumulative impacts that can reshape ecosystem dynamics and accelerate population declines of climate-sensitive species. Here, we use over two decades of rocky intertidal monitoring across 17 sites spanning over 1,200 km of coastline to assess how two unprecedented stressors—a multi-year marine heatwave and the disease-driven loss of a keystone predator (*Pisaster ochraceus*)—impacted populations of the canopy-forming intertidal kelp *Postelsia palmaeformis.* We show that *Postelsia* experienced rapid and severe declines during the 2014-2016 northeast Pacific marine heatwave, with an average population decline of 50%, multiple site-level extirpations, and particularly striking losses in the southern portion of the species' geographic range. Concurrently, *Pisaster* declines triggered mussel bed expansion into habitats previously occupied by *Postelsia*, further inhibiting kelp recoveries. Our findings reveal how converging stressors can drive persistent, broad-scale ecological shifts through both direct and indirect pathways. These results also highlight the critical role of long-term, spatially extensive monitoring in detecting and understanding global change impacts and provide a foundation for guiding *Postelsia* conservation and restoration efforts.

Keywords: Climate change, sea star wasting, sea palm, mussel, *Postelsia palmaeformis, Pisaster ochraceus*, *Mytilus californianus*

Data Availability Statement: This manuscript uses novel data and code that are publicly available at https://github.com/fgerraty/Postelsia_Collapse and archived via Zenodo at the following DOI: https://doi.org/10.5281/zenodo.16241083. Study site names and site coordinates are not included in publicly available data because *Postelsia palmaeformis* is a protected species and threatened by illegal human harvest.

1. Introduction:

Climate change is increasing the frequency and magnitude of extreme climatic events, such as heatwaves, wildfires, droughts, and floods, leading to profound consequences for ecological systems and human wellbeing (Newman and Noy 2023, Smith 2011). These acute, punctuated events often interact synergistically with long-term climatic changes or other stressors to drive extirpations, range shifts, and critical transitions from one ecosystem state to another. In the ocean, one of the most disruptive climate-driven phenomena is the increasing prevalence of marine heatwaves (MHWs)—prolonged periods of anomalously high ocean temperatures (Wernberg et al. 2013, Oliver et al. 2018, Marcos et al. 2025). MHWs trigger direct physiological stress in marine organisms and can generate cascading indirect effects through altered species interactions (Smith et al. 2023). They have been linked to local and regional declines or extinctions of critical foundation species (Miner et al. 2021, Starko et al. 2022, Wernberg et al. 2024), ecosystem regime shifts (Smith et al. 2024, Rogers-Bennett and Catton 2019), and devastating social and economic consequences (Smith et al. 2021, Free et al. 2023). With MHWs becoming more frequent, prolonged, and intense, they are likely to continue compounding the effects of other unprecedented stressors to reshape ecological and evolutionary dynamics across global oceans (Oliver et al. 2018).

Infectious disease outbreaks are also a growing threat for wildlife and can produce dramatic disruptions to community dynamics and ecosystem function. While the emergence and spread of wildlife diseases is often facilitated by human activities such as habitat modification, global trade, and pollution, climate change is also altering host-pathogen dynamics in complex ways (Altizer et al. 2013; Burge et al. 2014; Mahon et al. 2024). In some cases, warming temperatures may reduce disease risk (Cohen et al. 2020), but more often shifting environmental conditions exacerbate pathogen impacts on wildlife (Harvell et al., 2002, Mahon et al. 2024). This is particularly concerning for foundation species and keystone predators, where disease outbreaks can initiate trophic cascades that ripple through food webs and restructure ecosystems (Buck and Ripple 2017, Holdo et al. 2009, Moritsch 2021). The intersection of warming temperatures and wildlife disease has already led to widespread mortality events in tropical and temperate oceans, with consequences for ecosystem services as well as human health and wellbeing (Burge et al. 2014).

Beginning in 2013, an invertebrate epizootic known as sea star wasting disease (SSWD) devastated intertidal and nearshore sea star populations along the northeast Pacific coast from Mexico to Alaska (Harvell et al. 2019, Miner et al. 2018). The disease spread rapidly in 2013-2015, affecting at least 20 asteroid species and causing severe declines in several critical predators including the sunflower sea star (*Pycnopodia helianthoides*) and the ochre star (*Pisaster ochraceus*, hereafter *Pisaster*) (Hamilton et al. 2021, Hewson et al. 2025, Konar et al. 2019, Menge et al. 2016, Miner et al. 2018). Immediately following the SSWD outbreak, an unprecedented multi-year MHW—known as the 2014-2016 northeast Pacific MHW—extended from Baja California to the Gulf of Alaska and persisted from November 2013 to August 2016 (Di Lorenzo & Mantua, 2016). This event, the longest recorded MHW to date, drove broad-reaching ecological and social consequences including range shifts, mass mortality events, and fisheries closures (Cavole et al. 2016, Starko et al. 2025).

In northeast Pacific rocky subtidal and intertidal ecosystems, the confluence of the SSWD outbreak and the 2014-2016 MHW—two simultaneous and unprecedented stressors—has been associated with the collapse of subtidal kelp forests and expansion of urchin barrens (Burt et al. 2018, McPherson et al. 2021, Rogers-Bennett and Catton 2019, Schultz et al. 2016) as well as shifts from macrophyte- to invertebrate-dominated intertidal communities (Meunier et al. 2024, Traiger et al. 2022, Whalen et al. 2023). The loss of *Pisaster*, a keystone predator which regulates rocky intertidal communities by preying on the California mussel (*Mytilus californianus*; Paine 1966, Paine 1974), likely played an impactful role in these intertidal regime shifts via trophic cascades (Meunier et al. 2024).

Despite the widespread ecological impacts of these simultaneous disturbance events, their effects on intertidal canopy-forming kelps remain poorly understood. This is especially true for *Postelsia palmaeformis* (hereafter *Postelsia*), a culturally and economically important but critically understudied kelp that occupies wave-exposed rocky intertidal shores (Ainis et al. 2019, Thompson et al. 2010, Turner 2001). *Postelsia* has a patchy distribution (Dayton 1973), extremely limited dispersal capacity (Coyer et al. 1997; Kusumo et al. 2006; Paine et al. 2017), and is sensitive to elevated water temperatures (Lüning and Freshwater 1988, Muth et al. 2019, Young 1971)—all traits that may heighten its vulnerability to climate change (Csordas et al., 2024). In addition, *Postelsia* commonly occurs amongst beds of competitively dominant *M. californianus* mussels (Dayton 1973, Paine 1979), potentially making the species vulnerable to mussel bed expansion triggered by *Pisaster* losses.

Here, we examine the direct and indirect effects of the 2014-2016 MHW and the synergistic SSWD outbreak on the abundance, persistence, and recovery of *Postelsia*. To do so, we leverage long-term rocky intertidal community monitoring data collected for over two decades at seventeen sites spanning most of the southern portion of the kelp's geographic range. We hypothesized that *Postelsia* declined due to heat stress during the 2014-2016 MHW, and that *Pisaster* loss led to mussel bed expansion, indirectly hindering *Postelsia* recovery (Meunier et al. 2024). Consequently, we predicted that these synergistic disturbances acted as a "one-two punch" to drive persistent, broad-scale *Postelsia* declines.

2. Materials and methods:

2.1 Study System

We studied rocky intertidal communities at 17 sites that were established as part of the Multi-Agency Rocky Intertidal Network (MARINe, www.pacificrockyintertidal.org), a collaborative long-term monitoring program designed to capture natural dynamics and patterns of change in rocky intertidal communities along the Pacific Coast of North America. Our study region, spanning over 1,200 km of coastline from Central Oregon to Central California, USA (Figure 1), encompasses over half of the latitudinal distribution of *Postelsia* and includes the vast majority of the species' equatorial "trailing edge" of its geographic range. This annual brown alga, colloquially known as "sea palm," occurs along wave-exposed rocky intertidal shores from Central California, USA, to Cranston Point, British Columbia, Canada (Abbott and Hollenberg 1976, Z. Monteith personal communication).

Postelsia exhibits a patchy distribution at both broad and local spatial scales, with presence tightly linked to areas of extreme wave shock (Dayton 1973). This canopy forming species co-occurs in the mid-tidal zone with the mussel *Mytilus californianus* (Dayton 1973, Paine 1979). Due to its life-cycle, the sporophytic stage of *Postelsia*—the stage capable of defending space on the rock against mussel encroachment—is not present for several months each year (Paine 1979). Thus, successful recruitment of successive generations of sporophytes often depends on wave-induced disturbances (Blanchette 1996, Dayton 1973, Paine 1979, Paine 1988) and predation by *Pisaster* sea stars to open up space for colonization within mussel beds (Dayton 1971, Paine 1966, Paine 1974). However, while mussels will ultimately outcompete and exclude Postelsia in the absence of disturbance, mussel beds may also provide a protective microhabitat that enhances the survival of *Postelsia*'s microscopic stages during the fall and winter months (Blanchette 1996).

Spores generally settle within 2 m from their parent plant, and patches > 25 m apart typically show distinct genetic structure (Coyer et al. 1997; Kusumo et al. 2006; Paine et al. 2017). Long-distance dispersal events are thought to be exceedingly rare, limited to occasional floating individuals that have been ripped from the substratum (Paine et al. 2017). Thus, if *Postelsia* is locally extirpated from an area, as was observed for a population at the southern edge of the alga's range during the 1982-1983 ENSO event (Young 1971, J. Steinbeck personal communication), natural recovery might never occur.

Postelsia's habitat specificity, poor dispersal ability, and sensitivity to warm water temperatures, combined with its inferior competitive status with mussels, might make it particularly vulnerable to the combined effects of MHWs and keystone predator losses. However, apart from a recent investigation near the species' leading (cold-water) range edge (Vancouver Island, BC) that found long-term stability of *Postelsia* from 2006-2022 (Csordas et al. 2024), the impacts of these paired disturbances on *Postelsia* populations remains unknown.

2.2 Postelsia surveys

To monitor long-term changes in *Postelsia* abundance across a broad geographic scale, we established 1-3 permanent transects at each of 17 MARINe sites along the California and Oregon coastline (Figure 1). Fixed plots were established in areas where *Postelsia* was initially abundant and could be accessed safely. These plots typically consisted of 2 m-wide band transects delimited by bolts anchored to the substratum and varying in length from 5-20 m. We counted the total number of *Postelsia* within each band transect during each survey. To avoid issues with seasonality due to *Postelsia*'s annual life history, sites were generally sampled in the same period (i.e. a "canonical season") each year (March-April in Central California, May-June in Northern California, and July in Oregon). Some sites were surveyed in non-canonical seasons or multiple seasons in some years; in these cases, we only included surveys conducted in the site's canonical season for analyses.

To determine temporal dynamics, we first identified the year with the highest recorded *Postelsia* density at each site and expressed all other survey estimates at the site as a percentage of this maximum density. We then visualized mean annual trends in *Postelsia* density with a generalized additive mixed-effects model fit to these percent of maximum density values, with year as a smoothing term and site as a random effect (Figure 2A). The model was fit using restricted maximum likelihood (REML) using the gam function in the mgcv package in R (version 4.5.0; Wood 2011, R Core Team 2025). We then directly compared mean *Postelsia* densities between periods before the MHW (≤ 2014) vs. during and after the MHW (≥ 2015) to determine site-level and regional metrics of MHW population impact (Figure 1A). To assess population recoveries, we also compared mean *Postelsia* densities among three periods, before the MHW (≤ 2014), during the MHW (2015-2016), and after the MHW (≥ 2017), with a generalized linear mixed effects model with a tweedie distribution, log link function, and site as a random effect. The model was fit using the glmmTMB function in the glmmTMB package, and assumptions were checked using the DHARMa package (Brooks et al. 2017, Hartig 2022).

2.3 Water temperature

As part of the MARINe program, we measured intertidal water temperatures at 10 of the *Postelsia* monitoring sites (sites 1-3, 5, 8, 12-14, 16, and 17) using HOBO Pendant and TidbiT (v1 and v2) temperature loggers (Onset Computer Corporation, Bourne, Massachusetts, United States) housed in stainless steel mesh cages anchored to the substratum at the interface between middle and low intertidal zones. After downloading logger data, we extracted water temperatures on the basis of daily tidal cycles and removed any outlier temperatures. We calculated daily mean water temperature for each site by averaging all water temperature measurements, then determined the baseline temperature climatology and detected MHW events at each site using the HeatwaveR package (Schlegel and Smit, 2018). Following Hobday et al. 2016, MHWs were defined as warm water periods lasting 5 days or more above the 90th percentile relative to long-term, period-specific local climatology, and were categorized from moderate (Category I) to extreme (Category IV) based on heatwave intensity (Figure 3). Categories were based on multiples of the value represented by the difference between the local climatological mean and the climatological 90th percentile, with categories defined as “moderate” (Category I; 1-2× the local difference), “strong” (Category II; 2-3×), “severe” (Category III; 3-4×), and “extreme” (Category IV; > 4×) (Hobday et al. 2018).

We calculated the number of days per year within each heatwave category at all sites (Figure S1), and the mean number of days per year in each heatwave category across all sites (Figure 3C). Finally, we determined the total number of MHW days per year at each site (including all heatwave categories) and fitted a generalized additive mixed-effects model to these values with year as a smoothing term and site as a random effect using REML to visualize temporal trends (Figure 2A). There were temporal gaps in water temperature data at several sites due to temperature logger failure, malfunction, and loss (e.g., Figure S1, Figure S2), so we removed all sites with over 25 missing days of temperature monitoring in any given year prior to multi-site data summarization.

2.4 Repeated photos

At five sites (sites 3, 8, 12, 13, and 16), the abundance of *Postelsia* and mussels were quantified using panoramic photos taken from fixed locations adjacent to *Postelsia* transects (2 repeat panoramic photos at 2 sites, 1 panoramic photo at 3 sites). Using imaging software, a standardized box was drawn around the same location in each image, and *Postelsia* and mussel patches were manually outlined using heads-up digitization to determine percent cover within the box. We digitized 6-10 panoramic photos from each site (55 photos total) taken between 2012-2021. To visualize temporal shifts in *Postelsia* and mussel percent cover within these photos, we calculated the percentage of maximum abundance (maximum percent cover within box) for each photo, then fitted a generalized additive mixed effects model for each species with year as a smoothing term and transect as a random effect using REML (Figure 4).

2.5 Sea star and mussel surveys

Ochre stars (*Pisaster*) were counted and measured at 15 sites (sites 1-13, 16, and 17) within three irregularly-shaped plots (20-160 m^2) permanently established in areas of initially high *Pisaster* density (Miner et al., 2018). The "radius" of each *Pisaster* was measured as the distance from the center of the star to the tip of its longest ray, estimated to the nearest 10 mm for individuals > 7 mm. Stars 3-7 mm were grouped into a 5 mm radius bin, and those < 3 mm were not counted due to inconsistent detection.

To standardize sea star abundance estimates across years, we calculated *Pisaster* biomass at each site using the length-biomass conversion equation from Moritsch & Raimondi (2018). We converted counts and size structure to biomass because predator biomass is a more ecologically relevant proxy for predation pressure. We then identified the year with the highest recorded biomass at each site and expressed all other survey estimates as a percentage of this maximum. While this approach does not allow for direct comparisons of *Pisaster* density or biomass between sites due to plot irregularities, it enables comparisons of relative biomass trends within each site over time. To visualize *Pisaster* declines associated with SSWD, we fit a generalized additive mixed-effects model to the relative biomass estimates, using year as a smoothing term and site as a random effect using REML (Figure 2B). We then compared these relative biomass estimates among periods before the SSWD outbreak (≤ 2013), during the SSWD outbreak (2013-2016), and after the SSWD outbreak (≥ 2017) using a linear mixed effects model with site as a random effect. The model was fit using the lmer function in the lme4 package, and assumptions were checked using the DHARMa package (Bates et al. 2015, Hartig 2022).

To document shifts in mussel abundance associated with *Pisaster* loss at a larger scale than the repeated photos dataset described above, we used data from MARINe Coastal Biodiversity Surveys (CBS) to compare mussel percent cover and tidal height distribution among surveys before and after the SSWD outbreak. Of the 17 sites, only 13 had CBS surveys both before (≤ 2013) and after (≥ 2014) the SSWD outbreak; analyses were therefore limited to these sites (1, 3, 4, 6, 7-10, 12-14, 16, and 17). CBS are designed to capture the abundance and distribution of all common taxa, including mussels, across the intertidal zone at fixed locations within each site, allowing for assessment of change through time. A fixed, uniformly distributed grid was established at each site, consisting of 11 vertical parallel transect lines spaced 3 m apart, with approximately 100 points per transect distributed across the full tidal range, which resulted in approximately 1,100 points per site. Organisms under each point were identified to the lowest possible taxonomic level, including layering and epibionts when appropriate (see https://www.pacificrockyintertidal.org for full description of methods).

The upper elevational limit of mussels is restricted by temperature and desiccation, whereas the lower limit is regulated by *Pisaster* predation (Dayton 1971, Paine 1974). Because of this, we hypothesized that SSWD-driven *Pisaster* declines would cause mussels to (1) increase in percent cover across the intertidal and (2) expand to lower tidal heights at the lower edge of its vertical distribution. To assess changes in mussel percent cover between the periods before and after SSWD (≤ 2013 vs. 2014-2023; hypothesis 1), we determined the percent cover of *M. californianus* in each CBS survey (# *M. californianus* points/all survey points*100) and then fit a linear mixed-effects model with time period (pre/post SSWD) as a fixed effect and site as a random effect to these percent cover values. This model was fit using the lmer function in the lme4 package, and assumptions were checked using the DHARMa package (Bates et al.

2015, Hartig 2022). To assess shifts in the tidal height of the lower distributional limit of *M. californianus* before and after the SSWD outbreak, we first determined the tidal height of each mussel detection relative to mean lower low water (MLLW). This was done by integrating biological survey data with transect-level topographic profiles obtained using a rotating laser level. We then fit linear quantile mixed-effects models based on the asymmetric Laplace distribution, with time period (pre/post SSWD) as a fixed effect and transect as a random effect, to three quantiles of mussel tidal height distributions ($\tau = .1, .5$, and $.9$; i.e., 10th, 50th, and 90th percentiles) using the lqmm function in the lqmm package (Geraci 2014, Geraci and Bottai 2014). We used quantile regression because it allowed us to assess changes across the full distribution of mussel tidal heights—not just the mean—thereby capturing shifts in both the core and boundaries of the species' vertical range.

Importantly, permanent sea star monitoring plots and CBS grid locations do not always directly overlap with *Postelsia* permanent transects, but they are typically within 50 m and always within 200 m of one another.

2.6 Statistical analysis and visualization software

All analyses were conducted in R version 4.5.0 (R Core Team 2025) using the following packages: tidyverse (v2.0.0, Wickham et al. 2019), heatwaveR (v0.5.4, Schlegel and Smit 2018), mgcv (v1.9.1, Wood 2011), glmmTMB (v1.1.11, Brooks et al. 2017), DHARMa (v0.4.7, Hartig 2022), lme4 (v1.1-37, Bates et al. 2015), and lmqq (v1.5.8, Geraci 2014, Geraci and Bottai 2014). Figures and tables were generated using ggplot2 (v3.5.2, Wickham 2016), ggthemes (v5.1.0, Arnold 2021), sf (v1.0.20, Pebesma 2018), maps (v3.4.2.1, Becker et al. 2024), gratia (v0.10.0, Simpson 2024), gt (v1.0.0, Iannone et al. 2025), and biscale (v1.0.0, Prener et al. 2022). Data and code to reproduce all analyses and figures are publicly available (Gerraty et al. 2025).

3. Results:

We found evidence that the 2014-2016 MHW initiated severe, broad-scale *Postelsia* declines and that the synergistic SSWD outbreak indirectly hindered *Postelsia* recoveries (Figure 2). *Postelsia* abundance declined rapidly in 2014-2015 during the onset of the MHW, leading to local extirpations at the two southernmost sites (sites 16 and 17) and substantially reduced abundance in most other sites (Figure 1, Figure 2). Beginning in 2013, the SSWD outbreak led to sharp declines of *Pisaster*—a keystone predator—which was associated with an increase in mussel (*M. californianus)* abundance, mussel expansion to lower tidal heights, and mussel colonization of habitats formerly occupied by *Postelsia* (Figure 2, Figure 4, Figure 5).

3.1 Direct effects of marine heatwave

The northeast Pacific MHW began during summer 2014 and persisted through autumn 2016 in our study region. Although sub-regional variation was evident, the most intense period—based on temperature anomalies and the number of MHW days—occurred from September 2014 to April 2015 (Figure 3, Figure S1, Figure S2; Gentemann et al. 2017). After April 2015, water temperatures cooled in the northern portion of the study area, while the southern portion experienced another severe temperature spike from August to October 2015. Across sites with continuous temperature monitoring (< 25 days of temperature data missing per year), the mean number of MHW days was 110.6 in 2014 and 100.8 in 2015 (Figure 3C). Nine of 10 sites with water temperature loggers (excluding site 1) recorded maximum water temperatures exceeding 17 ºC (Table S1). Of these, five sites (sites 12-14, 16, 17) had maximum temperatures that exceeded 18 ºC, and one site (site 14) reached 20 ºC (Table S1). Most MHW events were classified as "moderate," but "strong" and "severe" events occurred at multiple sites in both years (Figure 3). One site (site 5) experienced an "extreme" MHW event in 2014, exceeding 4× the MHW threshold (Figure 3, Table S1).

Postelsia densities declined after the onset of the MHW at 13 out of 16 sites (81%) where pre-MHW (≤ 2014) and post-MHW (≥ 2015) surveys were conducted (Figure 1, Table S2). Across all sites, *Postelsia* densities declined by a mean of 49.6% between these periods. These declines often occurred rapidly after MHW onset, suggesting that anomalously warm water temperatures likely triggered direct physiological stress (Figure S3, Young 1971, Lüning and Freshwater 1988).

Declines in *Postelsia* were particularly pronounced in the southern portion of our study region; all sites south of Salmon Creek, Sonoma County (sites 11-17), exhibited >70% declines in density and local extirpations occurred at the two southernmost sites in 2015 (sites 16 and 17; Figure 1). Another site (site 13) experienced a local extirpation in 2016, but the population began to recover in 2018-2024, albeit to drastically lower densities than those documented prior to the MHW (Figure S3). Changes in *Postelsia* density were more variable north of Salmon Creek (sites 1-10), ranging from two sites with >90% declines to one site with a 75.5% increase in density (Figure 1, Table S2). However, the three sites with post-MHW density increases had limited sampling—only 1-2 surveys before the MHW, and just one survey after the MHW at two of three sites. Low sampling effort at these sites may have influenced our density change estimates due to stochastic variation (Figure S4).

Our generalized linear mixed-effects model comparing *Postelsia* density before (≤ 2014), during (2015-2016), and after (≥ 2017) the MHW provided strong evidence that density differed significantly among all time periods. *Postelsia* density was highest prior to the MHW (estimated marginal mean: 56.47 ± 7.09 SE individuals/m^2), declined sharply during the MHW (3.58 ± 1.02 SE), and partially rebounded post-MHW (12.09 ± 1.78 SE).

3.2 Indirect effects of sea star wasting

Sea star wasting was first documented in our study region in 2013, leading to rapid, significant declines in *Pisaster* biomass at all sites with high monitoring frequency except for site 8 (Miner et al. 2018; Figure 2B, Figure S5). Prior to the SSWD outbreak, *Pisaster* mean biomass was 60.4% ± 3.91 SE (estimated marginal mean) of the maximum biomass recorded in the sea star monitoring plots. In 2013-2016, after the onset of SSWD, *Pisaster* mean biomass collapsed to only 26.4% ± 5.34 SE of the maximum documented biomass. *Pisaster* populations began to rebound at most sites after 2016, although *Pisaster* biomass at a few—including the two southernmost sites—remain well below pre-SSWD levels (i.e., see sites 3, 16, and 17 in Figure S5). After 2016 (i.e., 2017-2024), *Pisaster* rebounded to 45.2% ± 3.85 SE of the maximum documented biomass. Importantly, biomass recovery does not necessarily mean the recovery of keystone predation pressure, particularly because a periodic absence of predation may allow mussels to grow beyond the size at which *Pisaster* can consume them (Paine 1976).

We found that *Pisaster* declines were temporally associated with increases in mussel abundance and mussel bed expansion to lower tidal heights. We conducted 51 CBS surveys at 13 sites between 2001 and 2023 to detect shifts in mussel abundance and distribution. Of these, 26 surveys occurred before the SSWD outbreak onset (≤ 2013), and 25 occurred after. The frequency and timing of CBS surveys varied among sites; for example, site 9 had only one survey before and one after the SSWD outbreak, whereas site 12 had five surveys before and three after. Across all CBS surveys, mussels (*M. californianus*) were detected at 12,499 survey points. Mussel percent cover increased significantly after the SSWD outbreak (estimate = 7.51% ± 1.05 SE, p < .001). Quantile regression revealed a significant lowering in the tidal height of the 10th and 50th (i.e., lower-elevation and median) percentiles of mussel distribution after the SSWD outbreak, with no significant change at the 90th percentile. At the 10th percentile ($\tau = .1$), mussels occurred significantly lower in the intertidal zone (estimate = –0.13 m ± .04 SE, $p < 0.001$), indicating a downward shift in the lower bounds of their vertical distribution. A similar but slightly smaller downward shift was observed at the median (estimate = –0.11 m ± .04 SE, $p = 0.012$). As expected, no significant change was detected at the 90th percentile (estimate = –0.03 ± .03 m SE, $p = 0.304$), suggesting that the upper tidal limit of mussels remained relatively stable following *Pisaster* declines.

Although sea star monitoring and CBS surveys provided compelling evidence that *Pisaster* declines were linked to increases in mussel abundance and mussel bed expansion to lower tidal heights, mechanistic detail on how these ecological shifts impacted *Postelsia* recoveries is limited due to the lack of direct overlap among sea star monitoring plots, CBS survey grids, and *Postelsia* transects. However, our repeated panoramic photos provided complementary insights into of how *Postelsia*-mussel interactions shifted during and after the MHW and SSWD outbreak. In 2012-2013, immediately prior to the MHW and SSWD outbreak, Postelsia mean cover was 81.4% ± 6.9 SE of the maximum percent cover in the repeated photos. By contrast, mean mussel cover was 28% ± 7.7 SE of its maximum percent cover. However, a dramatic shift occurred from 2014-2016, after which *Postelsia* mean cover dropped to 9.4% ± 3.1 SE of its maximum abundance and mussel mean cover expanded to 88% ± 2.5 SE of its maximum abundance (Figure 4, Figure S7). These data reveal that mussel beds expanded into areas previously occupied by *Postelsia* after the MHW and SSWD outbreak, thereby outcompeting *Postelsia* for space and limiting recoveries of remnant *Postelsia* populations.

4. Discussion:

Our study highlights how multiple, concurrent disturbance events can reshape population and community dynamics in strong and unexpected ways. We show that the 2014-2016 MHW was correlated with rapid and widespread *Postelsia* declines and that disease-driven *Pisaster* losses likely hindered kelp persistence and recovery by releasing competitively dominant mussels from keystone predation pressure (Figure 2). These results underscore the importance of considering both direct and indirect pathways when evaluating global change impacts on climate-sensitive species. Our findings also emphasize the critical role of long-term monitoring for detecting and understanding climate impacts and provide a foundation for guiding *Postelsia* conservation and management efforts.

4.1 Converging stressors

Ecological impacts of disturbance events tend to be studied in isolation, largely because acute perturbations have historically been rare, but global climate change and other anthropogenic stressors are increasing both the frequency and temporal overlap of extreme disturbances (Buma 2015, Newman and Noy 2023, Smith 2011). Our findings suggest that two simultaneous and unprecedented disturbance events—a MHW and a keystone predator disease outbreak—negatively impacted *Postelsia* through different mechanisms: the MHW caused direct physiological stress, while *Pisaster* declines indirectly limited kelp persistence and recovery by enabling the expansion of competitively dominant mussels into *Postelsia* habitats (Figure 2). While attribution of change is challenging during simultaneous disturbance events, is likely that the population-level impacts on *Postelsia* were more severe than would be expected if each disturbance had occurred independently. Forecasting long-term population dynamics for climate-sensitive species must therefore account for interactive and compounding effects of simultaneous disturbance events, such as those documented here (Buma 2015).

Warm water temperatures have long been considered as an important determinant of *Postelsia*'s southern distributional edge, despite an absence of field studies in the region documenting such associations (Young 1971, Lüning and Freshwater 1988). Laboratory studies have documented that *Postelsia* sporophytes are unable to withstand prolonged water temperatures >15 ºC, a value that roughly corresponds with the average maximum summer temperature at the southern range edge in San Luis Obispo county (Lüning and Freshwater 1988). In addition, Muth et al. (2019) found that *Postelsia* exhibited recruitment failure in a laboratory setting at 18 ºC. Every site with temperature loggers had more than 70 days where mean water temperatures exceeded 15 ºC, and the southernmost five of these sites had multiple days where water temperatures exceeded 18 ºC (Table S1). While lab-based thermal tolerance studies must be interpreted with caution because *Postelsia* likely exhibits local thermal adaptation due to its extremely limited dispersal, our findings are consistent with and build upon these results to suggest that climate-driven range retraction at *Postelsia*'s southern range edge is likely underway.

Identifying the interactive and cumulative impacts of both acute MHWs and chronic ocean warming on *Postelsia*'s distribution remains a critical research gap. A glimpse of historical insight is provided by Young (1971), which documented substantial *Postelsia* patches in one location at or near the kelp's southern range limit. However, all nearby patches were extirpated during the 1982-1983 ENSO event and have not recovered (J. Steinbeck personal communication). Documenting fine-scale distributional shifts and critical persistence thresholds, and also identifying the ecological and social consequences of *Postelsia* losses, are important research directions that can inform conservation and management strategies.

Our research adds to and is reinforced by a broad scientific understanding surrounding the negative impacts of MHWs on kelps in both subtidal and intertidal systems (Eger et al. 2024, Wernberg et al. 2024, Weitzman et al. 2021, Whalen et al. 2023). However, the cascading ecological consequences of disease outbreaks in predators have been less comprehensively documented, especially in marine ecosystems (Buck and Ripple 2017, Burge et al. 2014, Schultz et al. 2016). Our findings highlight how keystone predator losses can cascade through food webs to reshape population trajectories of climate-sensitive species. *Pisaster* losses were followed by increasing mussel abundance and mussel expansion to lower tidal heights, a result consistent with other studies documenting shifts from macroalgal to invertebrate-dominated intertidal communities during the SSWD outbreak and 2014-2016 MHW (Meunier et al. 2024, Traiger et al. 2022, Weitzman et al. 2021, Whalen et al. 2023). Mussels are a dominant competitor for space and can strongly influence rocky intertidal biodiversity and community composition (Miner et al. 2021, Paine 1974), so the negative ramifications of mussel bed expansion for

Poselsia persistence and recovery is likely just one of numerous ecological consequences arising in the aftermath of the SSWD outbreak. We encourage future research efforts to trace the diverse ecological legacies of SSWD-triggered *Pisaster* losses and explore how they continue to reshape coastal ecosystem dynamics into the present (Meunier et al. 2024, Smith et al. 2025).

4.2 Implications for conservation and management

Our findings of widespread and persistent *Postelsia* declines have direct implications for the management of this ecologically, economically, and culturally significant kelp. *Postelsia* is currently harvested for both commercial and recreational purposes, with regulations varying across its range depending on state or provincial jurisdiction. The most common harvesting practice is to trim blades above the meristem, which allows individuals to survive and blades to regrow, but this method can still reduce spore production and hinder recruitment (Thompson et al. 2010). Blade harvest after the onset of sporogenesis has been shown to sharply reduce spore production, suggesting that harvest timing is critical for sustainability of the *Postelsia* fishery (Thompson et al. 2010). To mitigate detrimental harvest impacts, potential management actions include mandating blade-trimming harvest methods, restricting harvest to a defined season that ends prior to the onset of sporogenesis, and establishing temporary or permanent closures for both recreational and commercial take in areas experiencing decline or where remnant populations are failing to recover (Thompson et al. 2010).

Because *Postelsia* disperses primarily over short distances, short-term recoveries in areas where local populations have been extirpated is unlikely without restoration interventions. Potential restoration efforts would therefore need to be targeted and conducted at local scales. *Postelsia* has been successfully transplanted via several methods (Paine 1979, Paine 1988, Nielsen et al. 2006, Paine et al. 2017), and transplanted *Postelsia* individuals have established local patches that persist for 5+ generations (Paine et al. 2017). Given the kelp's narrow habitat requirements (Paine 1988, Nielsen et al. 2006), careful site selection for restoration activities is essential for restoration success. Active clearing of mussels and other competitors from sites with transplanted or remnant populations may also improve restoration outcomes (Paine 1979, Paine 1988).

Critically, Indigenous peoples have harvested *Postelsia* for millennia, so any regulatory changes or conservation and restoration efforts should be developed in conversation and partnership with tribal communities and First Nations to support co-management and protect culturally significant practices (Ainis et al. 2019, Turner 2001, Van Pelt et al. 2017).

4.3 Importance of long-term, broad-scale ecosystem monitoring

Long-term, broad-scale ecological experiments and monitoring studies provide critical information about how global change influences biological communities and ecosystems (Hughes et al. 2017). These studies are increasingly important as anthropogenic stressors increase in diversity and intensity, often leading to interactive and cumulative emergent effects (Crain et al. 2008). In this study, we leverage data from 480 field surveys conducted from 1999-2024 at 17 field sites spanning over 1,200 km of coastline to show how converging stressors likely drove a ~50% decline in *Postelsia* populations across more than half of the species' geographic range. Studies spanning such broad spatial and temporal scales are rare, and therefore provide uniquely valuable insights into ecological and global change processes (Hughes et al. 2017).

Parsing long-term changes from stochastic ecological dynamics is less feasible for short-term studies or studies assessing population shifts at temporal snapshots separated by long periods (e.g., Csordas et al. 2024). In addition, many long-term monitoring studies solely examine population dynamics of single species instead of monitoring change across multiple taxa at varying trophic levels, thereby limiting inferences into the drivers of population changes (Coletti et al. 2016). Our ability to assemble multi-species monitoring datasets provided deeper understanding of the ecological processes underpinning *Postelsia* declines (Figure 2), which should hold significant weight in environmental policy and conservation and restoration decision making. We therefore urge strong and consistent investment in large-scale, long-term, multi-species monitoring programs because of the crucial ecological and management insights they provide, particularly as global change impacts intensify into the future (Hughes et al. 2017, Lindenmayer et al. 2022).

4.4 Limitations and future directions

Our results provide compelling evidence suggesting that direct physiological stress contributed to rapid *Postelsia* declines during the MHW and that SSWD indirectly limited *Postelsia* recoveries. However, our analyses remain correlative and we cannot fully disentangle causality due to the lack of experimental controls. In addition, while the *Postelsia* survey dataset we present here constitutes a majority of the species' long-term population monitoring data—particularly in our study region (but see Csordas et al. 2024 for long-term monitoring from Vancouver Island, BC)—the transects are small in spatial extent and may not fully capture broader-scale patterns of distributional change and recolonization dynamics (i.e., at scales from a rocky intertidal bench to an entire coastline). Moreover, because transect locations were selected in part based on their safe accessibility, the dataset may underrepresent more wave-exposed habitats where *Postelsia* population dynamics could differ. To address these gaps, future studies should pair long-term in situ monitoring with tools for surveying *Postelsia* abundance at broader spatial scales, such as with drones and aerial imaging (Csordas et al. 2024, Garza 2019). Experimental and modeling efforts are also needed to define critical thermal limits for *Postelsia* under realistic field conditions, to forecast *Postelsia* range contraction or distributional shifts, and to identify potential sites for targeted conservation and restoration efforts. Finally, deeper exploration of the social and ecological roles played by *Postelsia* can provide important insights into how kelp declines and potential recoveries influence social-ecological system dynamics.

4.4 Conclusions

Our study provides the most comprehensive assessment to date of *Postelsia* population dynamics across a large portion of the species' range, revealing severe and widespread declines linked to the combined impacts of the 2014-2016 MHW and SSWD-triggered *Pisaster* losses. By leveraging long-term, broad-scale, multi-species ecological monitoring, we demonstrate how concurrent disturbance events can interact to reshape the population dynamics of climate-sensitive species through both direct and indirect pathways. These findings underscore the need for conservation and management strategies that account for the complex, compounding, and interactive effects of global change.

Author Contributions

Francis D Gerraty: conceptualization, data curation, formal analysis, investigation, software, visualization, writing - original draft, writing - review and editing. **Karah N. Cox-Ammann:** conceptualization, investigation, writing - review and editing. **Melissa A. Douglas:** investigation, writing - review and editing. **Maya George:** investigation, writing - review and editing. **David P. Lohse:** conceptualization, data curation, formal analysis, investigation, writing - review and editing. **C. Melissa Miner:** data curation, investigation, writing - original draft, writing - review and editing. **Peter T. Raimondi:** conceptualization, formal analysis, funding acquisition, investigation, supervision, writing - review and editing.

Acknowledgements

This study utilized data collected by the Multi-Agency Rocky Intertidal Network (MARINe): a long-term ecological consortium funded and supported by many groups. Please visit pacificrockyintertidal.org for a complete list of the MARINe partners responsible for monitoring and funding these data. Special recognition should go to the agencies who have provided the majority of continuous funding for the project over several decades: Bureau of Ocean Energy Management, The National Park Service, The California Ocean Protection Council, and Partnership for Interdisciplinary Studies of Coastal Oceans. We are grateful to Rani Gaddam for data curation and interpretation, and Hallie Brown and Mike Grone for suggesting references. FDG was also supported by a NSF Graduate Research Fellowship and Achievement Rewards for College Scientists Fellowship.

Conflict of Interest Statement:

The authors declare no competing interests.

References

Abbott, L.A. and Hollenberg, L.G. (1976) Marine Algae of California Stanford. University Press, Stanford.

Ainis, A. F., Erlandson, J. M., Gill, K. M., Graham, M. H., & Vellanoweth, R. L. (2019). The Potential Use of Seaweeds and Marine Plants by Native Peoples of Alta and Baja California: Implications for "Marginal" Island Ecosystems. In A. F. Ainis, J. M. Erlandson, K. M. Gill, M. H. Graham, & R. L. Vellanoweth, *An Archaeology of Abundance* (pp. 135–170). University Press of Florida. https://doi.org/10.5744/florida/9780813056166.003.0005

Altizer, S., Ostfeld, R. S., Johnson, P. T. J., Kutz, S., & Harvell, C. D. (2013). Climate Change and Infectious Diseases: From Evidence to a Predictive Framework. *Science*, *341*(6145), 514–519. https://doi.org/10.1126/science.1239401

Arnold J (2021). ggthemes: Extra Themes, Scales and Geoms for 'ggplot2'. R package version 4.2.4, <https://CRAN.R-project.org/package=ggthemes>.

Bates D., Maechler, M., Bolker,B., Walker, S. (2015). Fitting Linear Mixed-Effects Models Using lme4. Journal of Statistical Software, 67(1), 1-48. doi:10.18637/jss.v067.i01.

Becker OScbRA, Minka ARWRvbRBEbTP, Deckmyn. A (2024). maps: Draw Geographical Maps. doi:10.32614/CRAN.package.maps <https://doi.org/10.32614/CRAN.package.maps>, R package version 3.4.2.1, <https://CRAN.R-project.org/package=maps>.

Blanchette, C. A. (1996). Seasonal patterns of disturbance influence recruitment of the sea palm, Postelsia palmaeformis. *Journal of Experimental Marine Biology and Ecology*, *197*(1), 1–14. https://doi.org/10.1016/0022-0981(95)00141-7

Buma, B. (2015). Disturbance interactions: Characterization, prediction, and the potential for cascading effects. *Ecosphere*, *6*(4), 1–15. https://doi.org/10.1890/ES15-00058.1

Buck, J. C., & Ripple, W. J. (2017). Infectious Agents Trigger Trophic Cascades. *Trends in Ecology & Evolution*, *32*(9), 681–694. https://doi.org/10.1016/j.tree.2017.06.009

Burge, C. A., Mark Eakin, C., Friedman, C. S., Froelich, B., Hershberger, P. K., Hofmann, E. E., Petes, L. E., Prager, K. C., Weil, E., Willis, B. L., Ford, S. E., & Harvell, C. D. (2014). Climate Change Influences on Marine Infectious Diseases: Implications for Management and Society. *Annual Review of Marine Science*, *6*(1), 249–277. https://doi.org/10.1146/annurev-marine-010213-135029

Brooks, M. E., K. Kristensen, K. J. van Benthem, A. Magnusson, C. W. Berg, A. Nielsen, H. J. Skaug, M. Maechler, and B. M. Bolker. 2017. "glmmTMB Balances Speed and Flexibility among Packages for Zero-Inflated Generalized Linear Mixed Modeling." The R Journal 9(2): 378–400. https://doi.org/10. 32614/RJ-2017-066.

Burt, J. M., Tinker, M. T., Okamoto, D. K., Demes, K. W., Holmes, K., & Salomon, A. K. (2018). Sudden collapse of a mesopredator reveals its complementary role in mediating rocky reef regime shifts. *Proceedings of the Royal Society B: Biological Sciences*, *285*(1883), 20180553. https://doi.org/10.1098/rspb.2018.0553

Cavole, L., Demko, A., Diner, R., Giddings, A., Koester, I., Pagniello, C., Paulsen, M.-L., Ramirez-Valdez, A., Schwenck, S., Yen, N., Zill, M., & Franks, P. (2016). Biological Impacts of the 2013–2015 Warm-Water Anomaly in the Northeast Pacific: Winners, Losers, and the Future. *Oceanography*, *29*(2). https://doi.org/10.5670/oceanog.2016.32

Cohen, J. M., Sauer, E. L., Santiago, O., Spencer, S., & Rohr, J. R. (2020). Divergent impacts of warming weather on wildlife disease risk across climates. *Science*, *370*(6519), eabb1702. https://doi.org/10.1126/science.abb1702

Coletti, H. A., Bodkin, J. L., Monson, D. H., Ballachey, B. E., & Dean, T. A. (2016). Detecting and inferring cause of change in an Alaska nearshore marine ecosystem. *Ecosphere*, *7*(10). https://doi.org/10.1002/ecs2.1489

Coyer, J. A., Ohen, J. L., & Stam, W. T. (1997). GENETIC VARIABILITY AND SPATIAL SEPARATION IN THE SEA PALM KELP *POSTELSIA PALMAEFORMIS* (PHAEOPHYCEAE) AS ASSESSED WITH M13 FINGERPRINTS AND RAPDS[1]. *Journal of Phycology*, *33*(4), 561–568. https://doi.org/10.1111/j.0022-3646.1997.00561.x

Crain, C. M., Kroeker, K., & Halpern, B. S. (2008). Interactive and cumulative effects of multiple human stressors in marine systems. *Ecology Letters*, *11*(12), 1304–1315. https://doi.org/10.1111/j.1461-0248.2008.01253.x

Csordas, M., Starko, S., Neufeld, C. J., Thompson, S. A., & Baum, J. K. (2024). Multiscale stability of an intertidal kelp (*Postelsia palmaeformis*) near its northern range edge through a period of prolonged heatwaves. *Annals of Botany*, *133*(1), 61–72. https://doi.org/10.1093/aob/mcad148

Dayton, P. K. (1971). Competition, Disturbance, and Community Organization: The Provision and Subsequent Utilization of Space in a Rocky Intertidal Community. *Ecological Monographs*, *41*(4), 351–389. https://doi.org/10.2307/1948498

Dayton, P. K. (1973). Dispersion, Dispersal, and Persistence of the Annual Intertidal Alga, Postelsia Palmaeformis Ruprecht. *Ecology*, *54*(2), 433–438. https://doi.org/10.2307/1934353

Di Lorenzo, E., & Mantua, N. (2016). Multi-year persistence of the 2014/15 North Pacific marine heatwave. *Nature Climate Change*, *6*(11), 1042–1047. https://doi.org/10.1038/nclimate3082

Eger, A. M., Eddy, N., McHugh, T. A., Arafeh-Dalmau, N., Wernberg, T., Krumhansl, K., Verbeek, J., Branigan, S., Kuwae, T., Caselle, J. E., Ospina, A. G., & Vergés, A. (2024). State of the world's kelp forests. *One Earth*, *7*(11), 1927–1931. https://doi.org/10.1016/j.oneear.2024.10.008

Free, C. M., Anderson, S. C., Hellmers, E. A., Muhling, B. A., Navarro, M. O., Richerson, K., Rogers, L. A., Satterthwaite, W. H., Thompson, A. R., Burt, J. M., Gaines, S. D., Marshall, K. N., White, J. W., & Bellquist, L. F. (2023). Impact of the 2014–2016 marine heatwave on US and Canada West Coast fisheries: Surprises and lessons from key case studies. *Fish and Fisheries*, *24*(4), 652–674. https://doi.org/10.1111/faf.12753

Garza, C. (2019). Landscape Ecology in the Rocky Intertidal: Opportunities for Advancing Discovery and Innovation in Intertidal Research. *Current Landscape Ecology Reports*, *4*(3), 83–90. https://doi.org/10.1007/s40823-019-00042-8

Gentemann, C. L., Fewings, M. R., & García-Reyes, M. (2017). Satellite sea surface temperatures along the West Coast of the United States during the 2014–2016 northeast Pacific marine heat wave. *Geophysical Research Letters*, *44*(1), 312–319. https://doi.org/10.1002/2016GL071039

Geraci M (2014). Linear Quantile Mixed Models: The lqmm Package for Laplace Quantile Regression. Journal of Statistical Software, 57(13), 1-29.

Geraci M and Bottai M (2014). Linear quantile mixed models. Statistics and Computing 24(3), 461-479.

Gerraty FD, Cox-Ammann KN, Douglas MA, George M, Lohse DP, Miner CM, Raimondi PT (2025). Fgerraty/Postelsia_Collapse: Marine heatwave and keystone predator loss drive broad-scale decline and hinder recovery of a rocky intertidal kelp (v0.0.1). Zenodo. https://doi.org/10.5281/zenodo.16241083

Hamilton, S. L., Saccomanno, V. R., Heady, W. N., Gehman, A. L., Lonhart, S. I., Beas-Luna, R., Francis, F. T., Lee, L., Rogers-Bennett, L., Salomon, A. K., & Gravem, S. A. (2021). Disease-driven mass mortality event leads to widespread extirpation and variable recovery potential of a marine predator across the eastern Pacific. *Proceedings of the Royal Society B: Biological Sciences*, *288*(1957), 20211195. https://doi.org/10.1098/rspb.2021.1195

Hartig, F. 2022. "DHARMa: Residual Diagnostics for Hierarchical (Multi-Level/Mixed) Regression Models." R Package Version 0.4.6, https://CRAN.R-project.org/package=DHARMa.

Harvell, C. D., Mitchell, C. E., Ward, J. R., Altizer, S., Dobson, A. P., Ostfeld, R. S., & Samuel, M. D. (2002). Climate Warming and Disease Risks for Terrestrial and Marine Biota. *Science*, *296*(5576), 2158–2162. https://doi.org/10.1126/science.1063699

Harvell, C. D., Montecino-Latorre, D., Caldwell, J. M., Burt, J. M., Bosley, K., Keller, A., Heron, S. F., Salomon, A. K., Lee, L., Pontier, O., Pattengill-Semmens, C., & Gaydos, J. K. (2019). Disease epidemic and a marine heat wave are associated with the continental-scale collapse of a pivotal predator (*Pycnopodia helianthoides*). *Science Advances*, *5*(1), eaau7042. https://doi.org/10.1126/sciadv.aau7042

Hewson, I., Johnson, M. R., & Reyes-Chavez, B. (2025). Lessons Learned from the Sea Star Wasting Disease Investigation. *Annual Review of Marine Science*, *17*(1), 257–279. https://doi.org/10.1146/annurev-marine-040623-082617

Hobday, A. J., Alexander, L. V., Perkins, S. E., Smale, D. A., Straub, S. C., Oliver, E. C. J., Benthuysen, J. A., Burrows, M. T., Donat, M. G., Feng, M., Holbrook, N. J., Moore, P. J., Scannell, H. A., Sen Gupta, A., & Wernberg, T. (2016). A hierarchical approach to defining marine heatwaves. *Progress in Oceanography*, *141*, 227–238. https://doi.org/10.1016/j.pocean.2015.12.014

Hobday, A., Oliver, E., Sen Gupta, A., Benthuysen, J., Burrows, M., Donat, M., Holbrook, N., Moore, P., Thomsen, M., Wernberg, T., & Smale, D. (2018). Categorizing and Naming Marine Heatwaves. *Oceanography*, *31*(2). https://doi.org/10.5670/oceanog.2018.205

Holdo, R. M., Sinclair, A. R. E., Dobson, A. P., Metzger, K. L., Bolker, B. M., Ritchie, M. E., & Holt, R. D. (2009). A Disease-Mediated Trophic Cascade in the Serengeti and its Implications for Ecosystem C. *PLoS Biology*, *7*(9), e1000210. https://doi.org/10.1371/journal.pbio.1000210

Hughes, B. B., Beas-Luna, R., Barner, A. K., Brewitt, K., Brumbaugh, D. R., Cerny-Chipman, E. B., Close, S. L., Coblentz, K. E., De Nesnera, K. L., Drobnitch, S. T., Figurski, J. D., Focht, B., Friedman, M., Freiwald, J., Heady, K. K., Heady, W. N., Hettinger, A., Johnson, A., Karr, K. A., … Carr, M. H. (2017). Long-Term Studies Contribute Disproportionately to Ecology and Policy. *BioScience*, *67*(3), 271–281. https://doi.org/10.1093/biosci/biw185

Iannone R, Cheng J, Schloerke B, Hughes E, Lauer A, Seo J, Brevoort K, Roy O (2025). gt: Easily Create Presentation-Ready Display Tables. doi:10.32614/CRAN.package.gt https://doi.org/10.32614/CRAN.package.gt, R package version 1.0.0, https://CRAN.R-project.org/package=gt

Konar, B., Mitchell, T. J., Iken, K., Coletti, H., Dean, T., Esler, D., Lindeberg, M., Pister, B., & Weitzman, B. (2019). Wasting disease and static environmental variables drive sea star assemblages in the Northern Gulf of Alaska. *Journal of Experimental Marine Biology and Ecology*, *520*, 151209. https://doi.org/10.1016/j.jembe.2019.151209

Kusumo, H. T., Pfister, C. A., & Wootton, J. T. (2006). Small-scale genetic structure in the sea palm Postelsia palmaeformis Ruprecht (Phaeophyceae). *Marine Biology*, *149*(4), 731–742. https://doi.org/10.1007/s00227-006-0254-z

Lindenmayer, D. B., Lavery, T., & Scheele, B. C. (2022). Why We Need to Invest in Large-Scale, Long-Term Monitoring Programs in Landscape Ecology and Conservation Biology. *Current Landscape Ecology Reports*, *7*(4), 137–146. https://doi.org/10.1007/s40823-022-00079-2

Lüning, K., & Freshwater, W. (1988). Temperature Tolerance of Northeast Pacific Marine Algae. *Journal of Phycology*, *24*(3), 310–315. https://doi.org/10.1111/j.1529-8817.1988.tb04471.x

Marcos M., Amores A., Agulles M., Robson J., & Feng X. (2025). Global warming drives a threefold increase in persistence and 1 °C rise in intensity of marine heatwaves, *Proceedings of the National Academy of Sciences*. 122 (16) e2413505122. https://doi.org/10.1073/pnas.2413505122

Mahon, M. B., Sack, A., Aleuy, O. A., Barbera, C., Brown, E., Buelow, H., Civitello, D. J., Cohen, J. M., De Wit, L. A., Forstchen, M., Halliday, F. W., Heffernan, P., Knutie, S. A., Korotasz, A., Larson, J. G., Rumschlag, S. L., Selland, E., Shepack, A., Vincent, N., & Rohr, J. R. (2024). A meta-analysis on global change drivers and the risk of infectious disease. *Nature*, *629*(8013), 830–836. https://doi.org/10.1038/s41586-024-07380-6

McPherson, M. L., Finger, D. J. I., Houskeeper, H. F., Bell, T. W., Carr, M. H., Rogers-Bennett, L., & Kudela, R. M. (2021). Large-scale shift in the structure of a kelp forest ecosystem co-occurs with an epizootic and marine heatwave. *Communications Biology*, *4*(1), 298. https://doi.org/10.1038/s42003-021-01827-6

Menge, B. A., Cerny-Chipman, E. B., Johnson, A., Sullivan, J., Gravem, S., & Chan, F. (2016). Sea Star Wasting Disease in the Keystone Predator Pisaster ochraceus in Oregon: Insights into Differential Population Impacts, Recovery, Predation Rate, and Temperature Effects from Long-Term Research. *PLOS ONE*, *11*(5), e0153994. https://doi.org/10.1371/journal.pone.0153994

Meunier, Z. D., Hacker, S. D., & Menge, B. A. (2024). Regime shifts in rocky intertidal communities associated with a marine heatwave and disease outbreak. *Nature Ecology & Evolution*, *8*(7), 1285–1297. https://doi.org/10.1038/s41559-024-02425-5

Miner, C. M., Burnaford, J. L., Ambrose, R. F., Antrim, L., Bohlmann, H., Blanchette, C. A., Engle, J. M., Fradkin, S. C., Gaddam, R., Harley, C. D. G., Miner, B. G., Murray, S. N., Smith, J. R., Whitaker, S. G., & Raimondi, P. T. (2018). Large-scale impacts of sea star wasting disease (SSWD) on intertidal sea stars and implications for recovery. *PLOS ONE*, *13*(3), e0192870. https://doi.org/10.1371/journal.pone.0192870

Miner, C. M., Burnaford, J. L., Ammann, K., Becker, B. H., Fradkin, S. C., Ostermann-Kelm, S., Smith, J. R., Whitaker, S. G., & Raimondi, P. T. (2021). Latitudinal variation in long-term stability of North American rocky intertidal communities. *Journal of Animal Ecology*, *90*(9), 2077–2093. https://doi.org/10.1111/1365-2656.13504

Moritsch, M.M. (2021). Expansion of intertidal mussel beds following disease-driven reduction of a keystone predator. *Marine Environmental Research*, *169*, 105363. https://doi.org/10.1016/j.marenvres.2021.105363

Moritsch, M. M., & Raimondi, P. T. (2018). Reduction and recovery of keystone predation pressure after disease-related mass mortality. *Ecology and Evolution*, *8*(8), 3952–3964. https://doi.org/10.1002/ece3.3953

Muth, A. F., Graham, M. H., Lane, C. E., & Harley, C. D. G. (2019). Recruitment tolerance to increased temperature present across multiple kelp clades. *Ecology*, *100*(3), e02594. https://doi.org/10.1002/ecy.2594

Newman, R., & Noy, I. (2023). The global costs of extreme weather that are attributable to climate change. *Nature Communications*, *14*(1), 6103. https://doi.org/10.1038/s41467-023-41888-1

Nielsen, K. J., Blanchette, C. A., Menge, B. A., & Lubchenco, J. (2006). PHYSIOLOGICAL SNAPSHOTS REFLECT ECOLOGICAL PERFORMANCE OF THE SEA PALM, *POSTELSIA PALMAEFORMIS* (PHAEOPHYCAEA) ACROSS INTERTIDAL ELEVATION AND EXPOSURE GRADIENTS. *Journal of Phycology*, *42*(3), 548–559. https://doi.org/10.1111/j.1529-8817.2006.00223.x

Oliver, E. C. J., Donat, M. G., Burrows, M. T., Moore, P. J., Smale, D. A., Alexander, L. V., Benthuysen, J. A., Feng, M., Sen Gupta, A., Hobday, A. J., Holbrook, N. J., Perkins-Kirkpatrick, S. E., Scannell, H. A., Straub, S. C., & Wernberg, T. (2018). Longer and more frequent marine heatwaves over the past century. *Nature Communications*, *9*(1), 1324. https://doi.org/10.1038/s41467-018-03732-9

Paine, R. T. (1966). Food Web Complexity and Species Diversity. *The American Naturalist*, *100*(910), 65–75. https://doi.org/10.1086/282400

Paine, R. T. (1974). Intertidal community structure: Experimental studies on the relationship between a dominant competitor and its principal predator. *Oecologia*, *15*(2), 93–120. https://doi.org/10.1007/BF00345739

Paine, R. T. (1976). Size-Limited Predation: An Observational and Experimental Approach with the Mytilus-Pisaster Interaction. *Ecology*, *57*(5), 858–873. https://doi.org/10.2307/1941053

Paine, R. T. (1979). Disaster, Catastrophe, and Local Persistence of the Sea Palm *Postelsia palmaeformis*. *Science*, *205*(4407), 685–687. https://doi.org/10.1126/science.205.4407.685

Paine, R. T. (1988). Habitat Suitability and Local Population Persistence of the Sea Palm Postelsia Palmaeformis. *Ecology*, *69*(6), 1787–1794. https://doi.org/10.2307/1941157

Paine, R. T., Buhle, E. R., Levin, S. A., & Kareiva, P. (2017). Short-range dispersal maintains a volatile marine metapopulation: The brown alga *Postelsia palmaeformis*. *Ecology*, *98*(6), 1560–1573. https://doi.org/10.1002/ecy.1798

Pebesma, E., 2018. Simple Features for R: Standardized Support for Spatial Vector Data. The R Journal 10 (1), 439-446, https://doi.org/10.32614/RJ-2018-009

Prener C, Grossenbacher T, Zehr A (2022). biscale: Tools and Palettes for Bivariate Thematic Mapping. R package version 1.0.0. https://doi.org/10.32614/CRAN.package.biscale

R Core Team (2025). R: A Language and Environment for Statistical Computing. R Foundation for Statistical Computing, Vienna, Austria. <https://www.R-project.org/>.

Rogers-Bennett, L., & Catton, C. A. (2019). Marine heat wave and multiple stressors tip bull kelp forest to sea urchin barrens. *Scientific Reports*, *9*(1), 15050. https://doi.org/10.1038/s41598-019-51114-y

Schlegel RW, Smit AJ (2018). “heatwaveR: A central algorithm for the detection of heatwaves and cold-spells.” Journal of Open Source Software, *3*(27), 821. https://doi.org/10.21105/joss.00821

Schultz, J. A., Cloutier, R. N., & Côté, I. M. (2016). Evidence for a trophic cascade on rocky reefs following sea star mass mortality in British Columbia. *PeerJ*, *4*, e1980. https://doi.org/10.7717/peerj.1980

Simpson G (2024). gratia: Graceful ggplot-Based Graphics and Other Functions for GAMs Fitted using mgcv. R package version 0.10.0, https://gavinsimpson.github.io/gratia/

Smith, J. G., Malone, D., & Carr, M. H. (2024). Consequences of kelp forest ecosystem shifts and predictors of persistence through multiple stressors. *Proceedings of the Royal Society B: Biological Sciences*, *291*(2016), 20232749. https://doi.org/10.1098/rspb.2023.2749

Smith, J. G., Fujii, J. A., Gaddam, R., Konrad, L., Lyon, S., Nicholson, T. E., Raimondi, P. T., Ridlon, A. D., Staedler, M., Tomoleoni, J. A., Yee, J. L., & Tinker, M. T. (2025). Keystone interdependence: Sea otter responses to a prey surplus following the collapse of a rocky intertidal predator. *Science Advances*, *11*(18), eadu1028. https://doi.org/10.1126/sciadv.adu1028

Smith, K. E., Burrows, M. T., Hobday, A. J., King, N. G., Moore, P. J., Sen Gupta, A., Thomsen, M. S., Wernberg, T., & Smale, D. A. (2023). Biological Impacts of Marine Heatwaves. *Annual Review of Marine Science*, *15*(1), 119–145. https://doi.org/10.1146/annurev-marine-032122-121437

Smith, K. E., Burrows, M. T., Hobday, A. J., Sen Gupta, A., Moore, P. J., Thomsen, M., Wernberg, T., & Smale, D. A. (2021). Socioeconomic impacts of marine heatwaves: Global issues and opportunities. *Science*, *374*(6566), eabj3593. https://doi.org/10.1126/science.abj3593

Smith, M. D. (2011). The ecological role of climate extremes: Current understanding and future prospects. *Journal of Ecology*, *99*(3), 651–655. https://doi.org/10.1111/j.1365-2745.2011.01833.x

Starko, S., Epstein, G., Chalifour, L., Bruce, K., Buzzoni, D., Csordas, M., ... & Baum, J. K. (2025). Ecological responses to extreme climatic events: a systematic review of the 2014-2016 Northeast Pacific marine heatwave. *Oceanogr. Mar. Biol. Annu. Rev.*

Starko, S., Neufeld, C. J., Gendall, L., Timmer, B., Campbell, L., Yakimishyn, J., Druehl, L., & Baum, J. K. (2022). Microclimate predicts kelp forest extinction in the face of direct and indirect marine heatwave effects. *Ecological Applications*, *32*(7), e2673. https://doi.org/10.1002/eap.2673

Thompson, S., Knoll, H., Blanchette, C., & Nielsen, K. (2010). Population consequences of biomass loss due to commercial collection of the wild seaweed Postelsia palmaeformis. *Marine Ecology Progress Series*, *413*, 17–32. https://doi.org/10.3354/meps08705

Traiger, S. B., Bodkin, J. L., Coletti, H. A., Ballachey, B., Dean, T., Esler, D., Iken, K., Konar, B., Lindeberg, M. R., Monson, D., Robinson, B., Suryan, R. M., & Weitzman, B. P. (2022). Evidence of increased mussel abundance related to the Pacific marine heatwave and sea star wasting. *Marine Ecology*. https://doi.org/10.1111/maec.12715

Turner, N. J. (2001). “Coastal peoples and marine plants on the Northwest Coast,” in *Proceedings of the International Association of Aquatic and Marine Science Libraries and Information Centers*. Victoria, British Columbia.

Van Pelt, M., Steinruck, J., Laucci, R., Rosales, H., Rohde, J., Sinkyone Council Member Tribes, Sundberg, R., Ben, J., Comet, S., Torma, T., Hernandez, T., Chen, C., and Seminara, D. (2017) Informing the North Coast MPA Baseline: Traditional Ecological Knowledge of Keystone Marine Species and Ecosystems, A Collaborative Project Among: Tolowa Dee-ni’ Nation, InterTribal Sinkyone Wilderness Council, Cher-Ae Heights Indian Community of the Trinidad Rancheria, and Wiyot Tribe, May 2017. California Sea Grant, U.C. San Diego. https://caseagrant.ucsd.edu/sites/default/files/39-Rocha-Final.pdf

Weitzman, B., Konar, B., Iken, K., Coletti, H., Monson, D., Suryan, R., Dean, T., Hondolero, D., & Lindeberg, M. (2021). Changes in Rocky Intertidal Community Structure During a Marine Heatwave in the Northern Gulf of Alaska. *Frontiers in Marine Science*, *8*, 556820. https://doi.org/10.3389/fmars.2021.556820

Wernberg, T., Smale, D. A., Tuya, F., Thomsen, M. S., Langlois, T. J., De Bettignies, T., Bennett, S., & Rousseaux, C. S. (2013). An extreme climatic event alters marine ecosystem structure in a global biodiversity hotspot. *Nature Climate Change*, *3*(1), 78–82. https://doi.org/10.1038/nclimate1627

Wernberg, T., Thomsen, M. S., Baum, J. K., Bishop, M. J., Bruno, J. F., Coleman, M. A., Filbee-Dexter, K., Gagnon, K., He, Q., Murdiyarso, D., Rogers, K., Silliman, B. R., Smale, D. A., Starko, S., & Vanderklift, M. A. (2024). Impacts of Climate Change on Marine Foundation Species. *Annual Review of Marine Science*, *16*(1), 247–282. https://doi.org/10.1146/annurev-marine-042023-093037

Whalen, M. A., Starko, S., Lindstrom, S. C., & Martone, P. T. (2023). Heatwave restructures marine intertidal communities across a stress gradient. *Ecology*, *104*(5), e4027. https://doi.org/10.1002/ecy.4027

Wickham H, Averick M, Bryan J, Chang W, McGowan LD, François R, Grolemund G, Hayes A, Henry L, Hester J, Kuhn M, Pedersen TL, Miller E, Bache SM, Müller K, Ooms J, Robinson D, Seidel DP, Spinu V, Takahashi K, Vaughan D, Wilke C, Woo K, Yutani H (2019). “Welcome to the tidyverse.” Journal of Open Source Software, 4(43), 1686. doi:10.21105/joss.01686 <https://doi.org/10.21105/joss.01686>.

Wickham H. ggplot2: Elegant Graphics for Data Analysis. Springer-Verlag New York, 2016.

Wood, S.N. (2011) Fast stable restricted maximum likelihood and marginal likelihood estimation of semiparametric generalized linear models. Journal of the Royal Statistical Society (B) 73(1):3-36

Young, D. N. (1971). *Autoecology of postelsia palmaeformis in san luis obispo county, california* (Order No. 29336503). Available from ProQuest Dissertations & Theses A&I. (2691798480). Retrieved from https://www.proquest.com/dissertations-theses/autoecology-em-postelsia-palmaeformis-san-luis/docview/2691798480/se-2

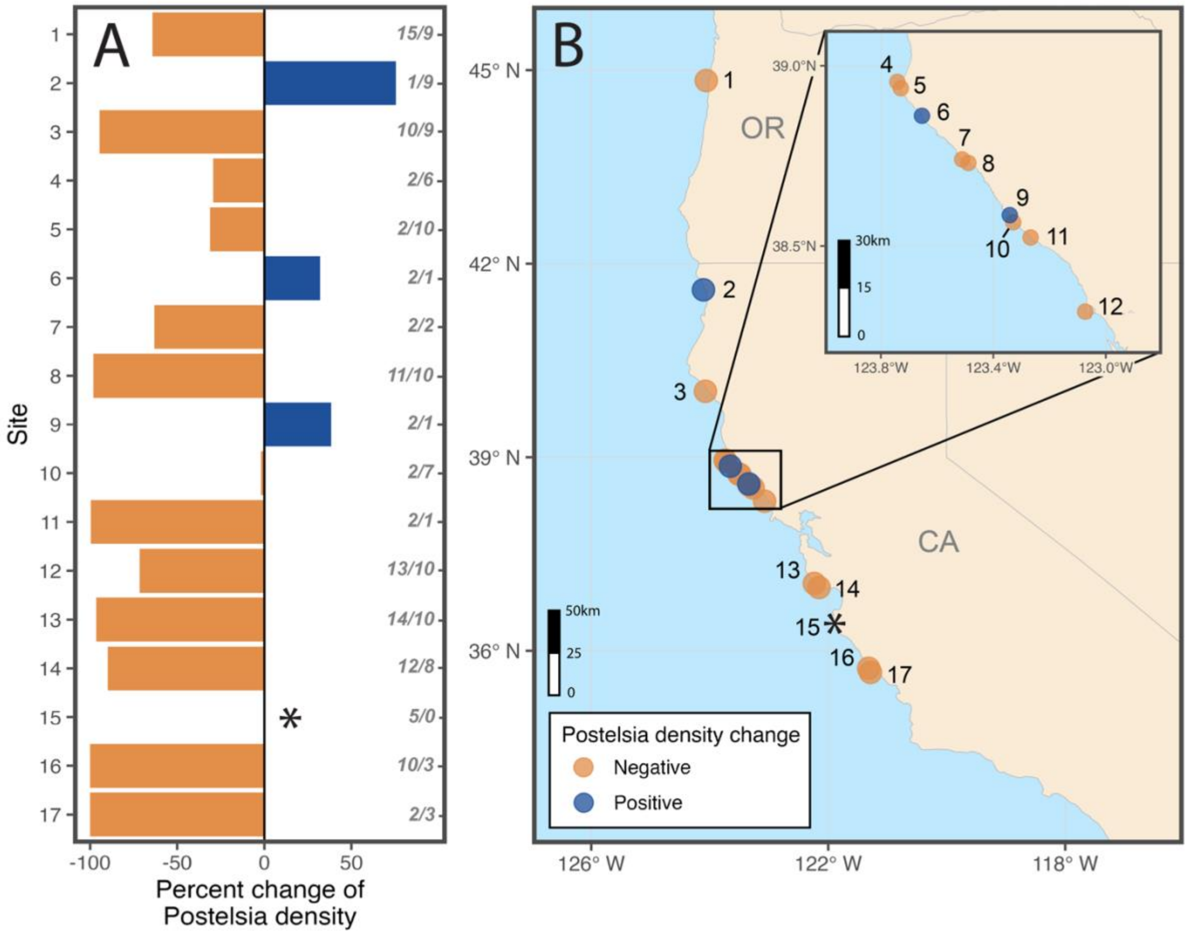

Figure 1. (A) Patterns of change in *Postelsia* density associated with the 2014-2016 northeast Pacific MHW. Bars display the change in mean densities at each site between *Postelsia* surveys before (≤ 2014) versus during and after (≥ 2015) the MHW. Gray, italicized numbers indicate the number of *Postelsia* surveys before / during and after the MHW. **(B)** Locations of *Postelsia* long-term monitoring sites in California and Oregon. Orange bars **(A)** and circles **(B)** indicate post-MHW declines in *Postelsia* density and blue bars/circles indicate post-MHW density increases. *No *Postelsia* surveys were conducted post-MHW at one site and density changes could therefore not be determined.

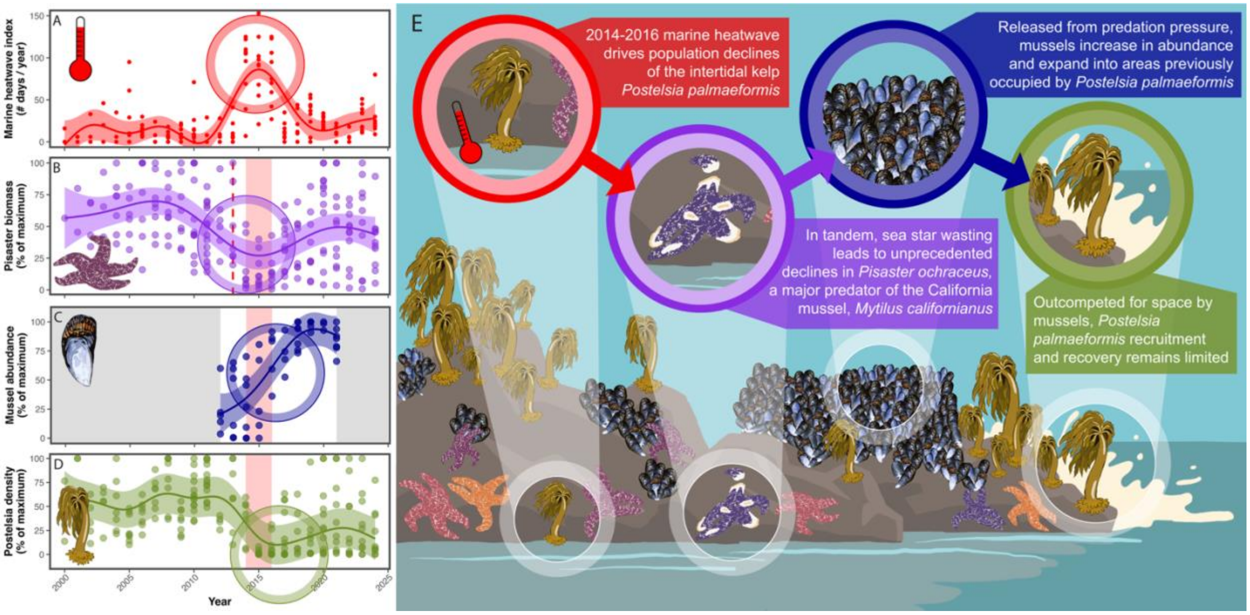

Figure 2. Progression of events affecting *Postelsia* abundance and temporal changes in the abundance of *Pisaster,* mussels (*M. californianus*), and *Postelsia*. **(A)** Total number of MHW days per year at each site with intertidal water temperature loggers (including all heatwave categories), **(B)** *Pisaster* biomass in sea star monitoring plots, **(C)** mussel percent cover from panoramic photos at *Postelsia* transects, and **(D)** *Postelsia* abundance—all modeled with generalized additive mixed-effects model with year as a smoothing term and site (or transect for mussels) as a random effect. Shaded pink region in panels **(B-D)** represents the 2014-2016 MHW and the red, vertical dashed line in panel **(B)** represents the onset of the SSWD outbreak. **(E)** Key events and ecological factors influencing *Postelsia* abundance. Illustration © Francis D Gerraty.

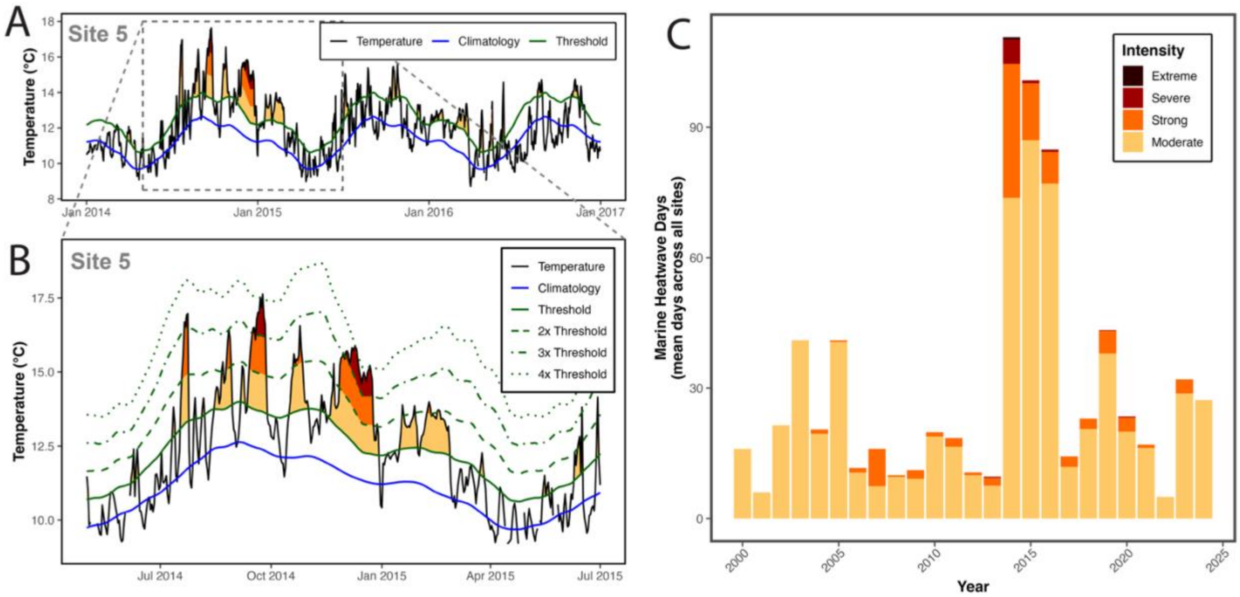

Figure 3. Intertidal water temperatures measured in rocky intertidal zones during the 2014-2016 MHW. **(A)** Water temperature at one site (site 5) throughout the MHW. When water temperatures (black line) exceeded the 90th percentile (green solid line) relative to the local long-term climatology (blue line) for five or more days, then MHW events were detected (colored fills). MHW events were categorized based on how much the temperature exceeded this threshold (moderate = 1-2×, strong = 2-3×, severe = 3-4×, extreme = >4×). Panel **(B)** shows these categorical thresholds and provides detail of the most extreme portion of the MHW at site 5. **(C)** Mean number of days per year across all sites that fell within each MHW category.

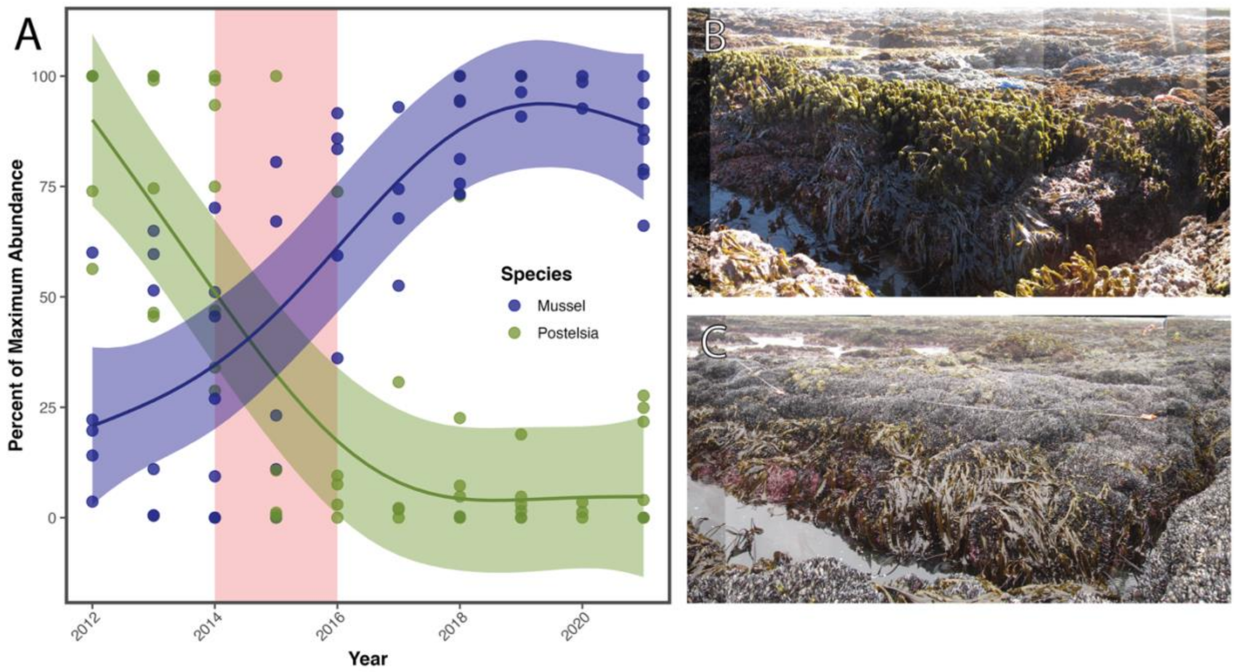

Figure 4. (A) Temporal changes in the abundance (maximum percent cover within standardized box) of *Postelsia* and mussels (*M. californianus*) in repeated panoramic photos. *Postelsia* and mussel cover in each photo was modeled with a generalized additive mixed effects model (for each species) with year as a smoothing term and transect as a random effect. Photographic examples of panoramic photos at site 3 before **(B)** and after **(C)** the 2014-2016 MHW.

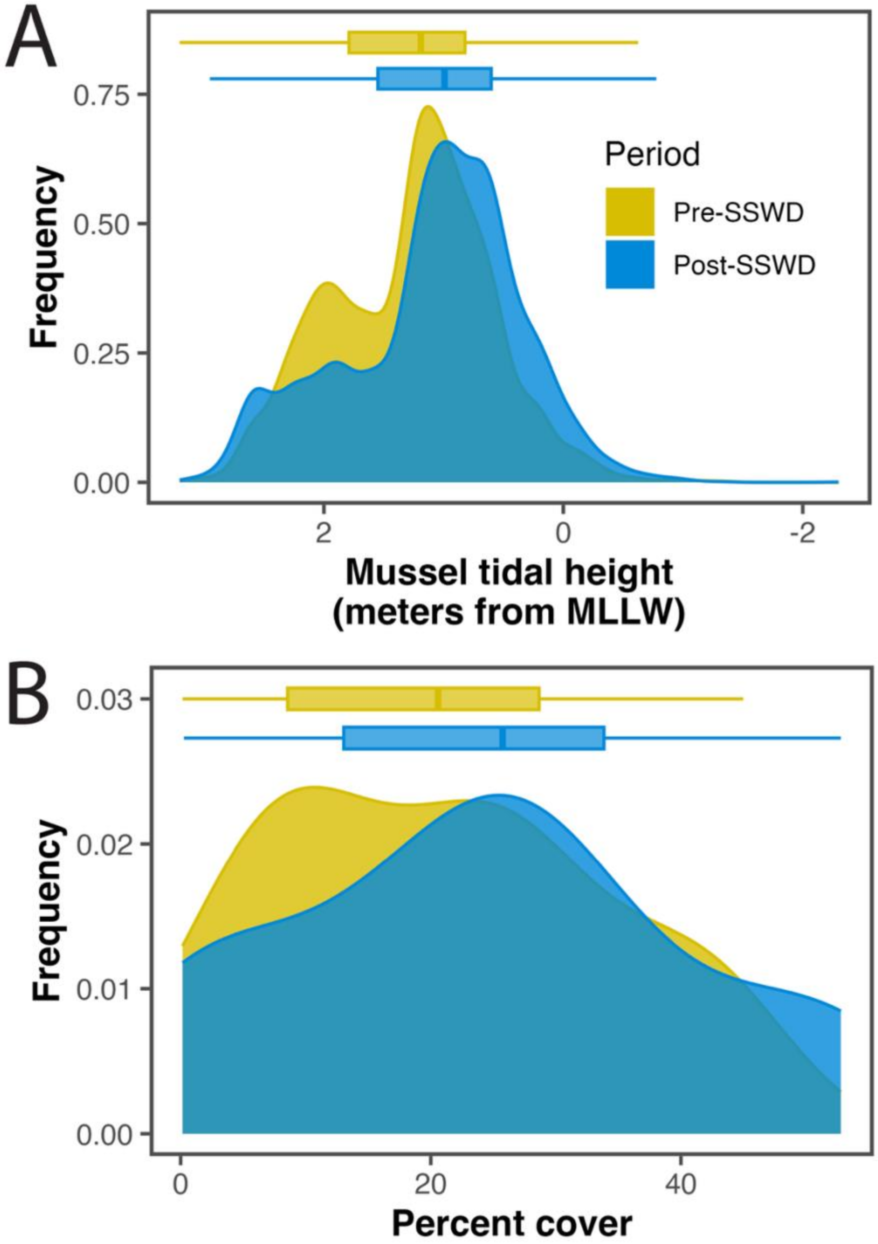

Figure 5. Changes in mussel (*M. californianus*) tidal height distribution **(A)** and frequency of percent cover at the site-wide scale **(B)** before (≤ 2013) and after (≥ 2014) the SSWD outbreak.

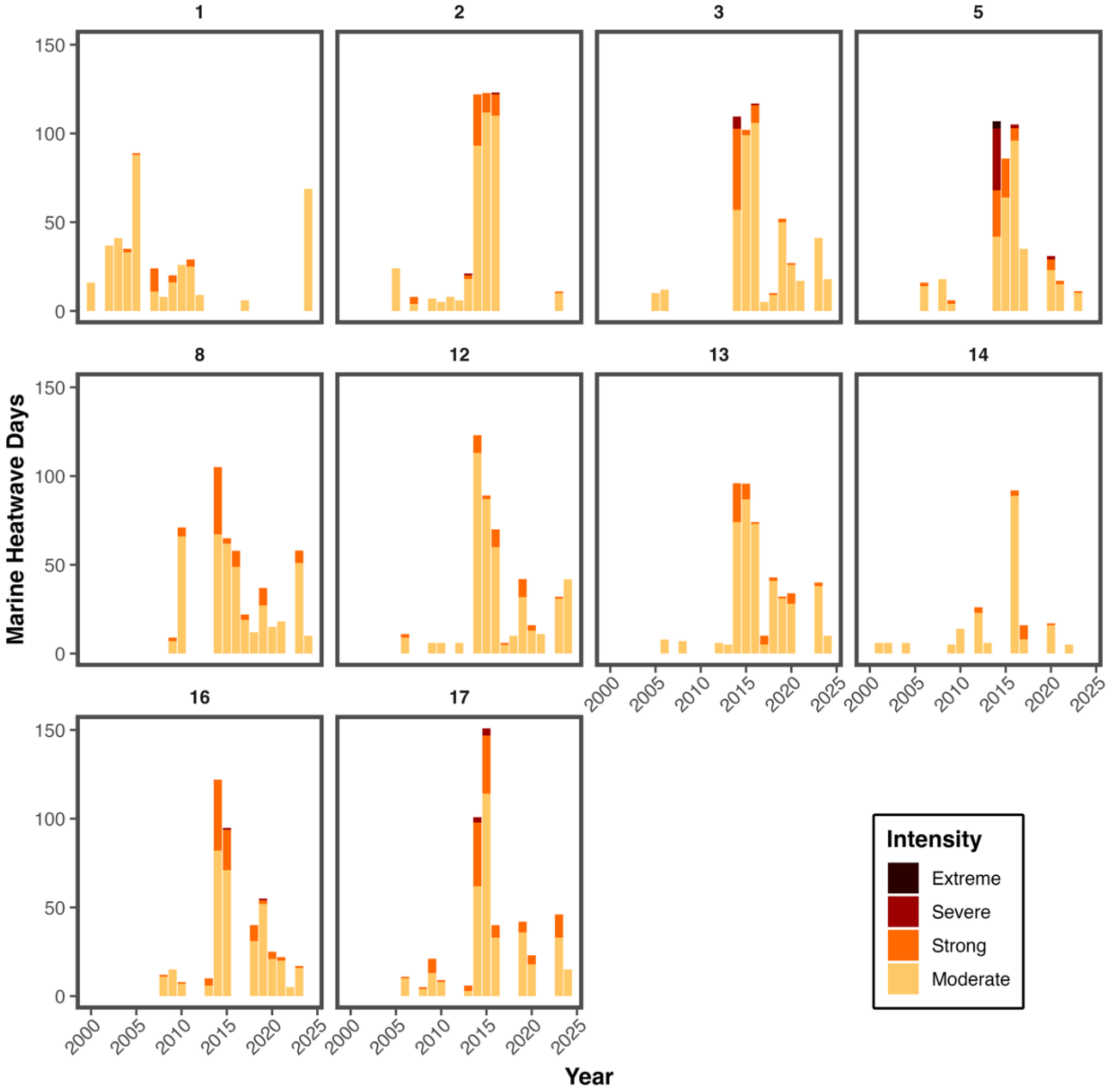

Figure S1. Number of days per year across all sites that fell within each MHW category. MHWs were defined as warm water periods lasting ≥5 days above the 90th percentile of long-term local climatology and categorized by the magnitude above this threshold: "moderate" (1-2×), "strong" (2-3×), "severe" (3-4×), and "extreme" (>4×). Note that gaps in water temperature data reflect variation in site visit frequency and temperature logger failure, malfunction, and loss.

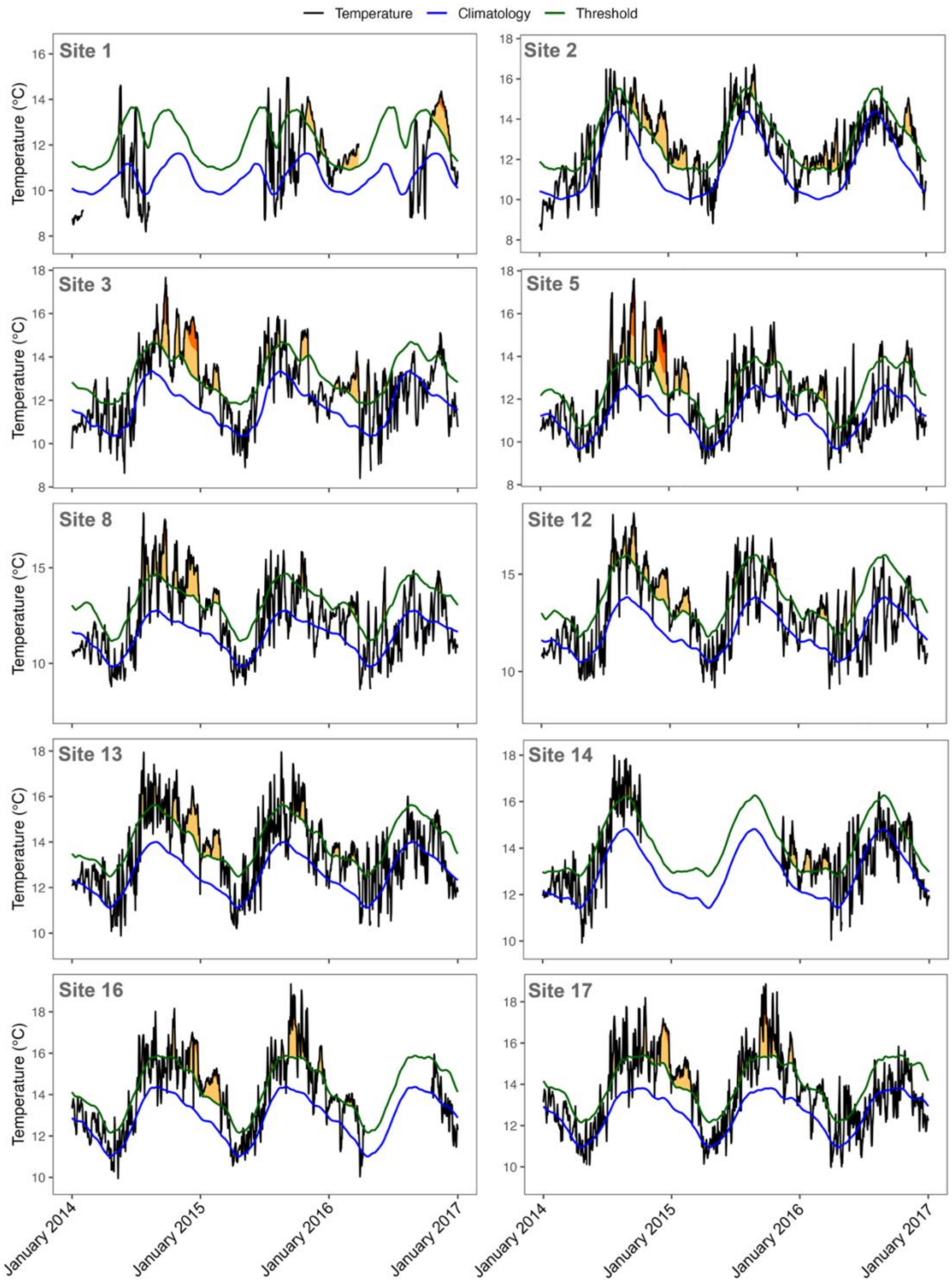

Figure S2. Intertidal water temperatures measured in rocky intertidal zones during the 2014-2016 MHW at all study sites with water temperature loggers. When water temperatures (black line) exceeded the 90th percentile (green solid line) relative to the local long-term climatology (blue line) for five or more days, then MHW events were detected (colored fills). Note that some sites did not have water temperature data due to due to temperature logger failure, malfunction, and loss.

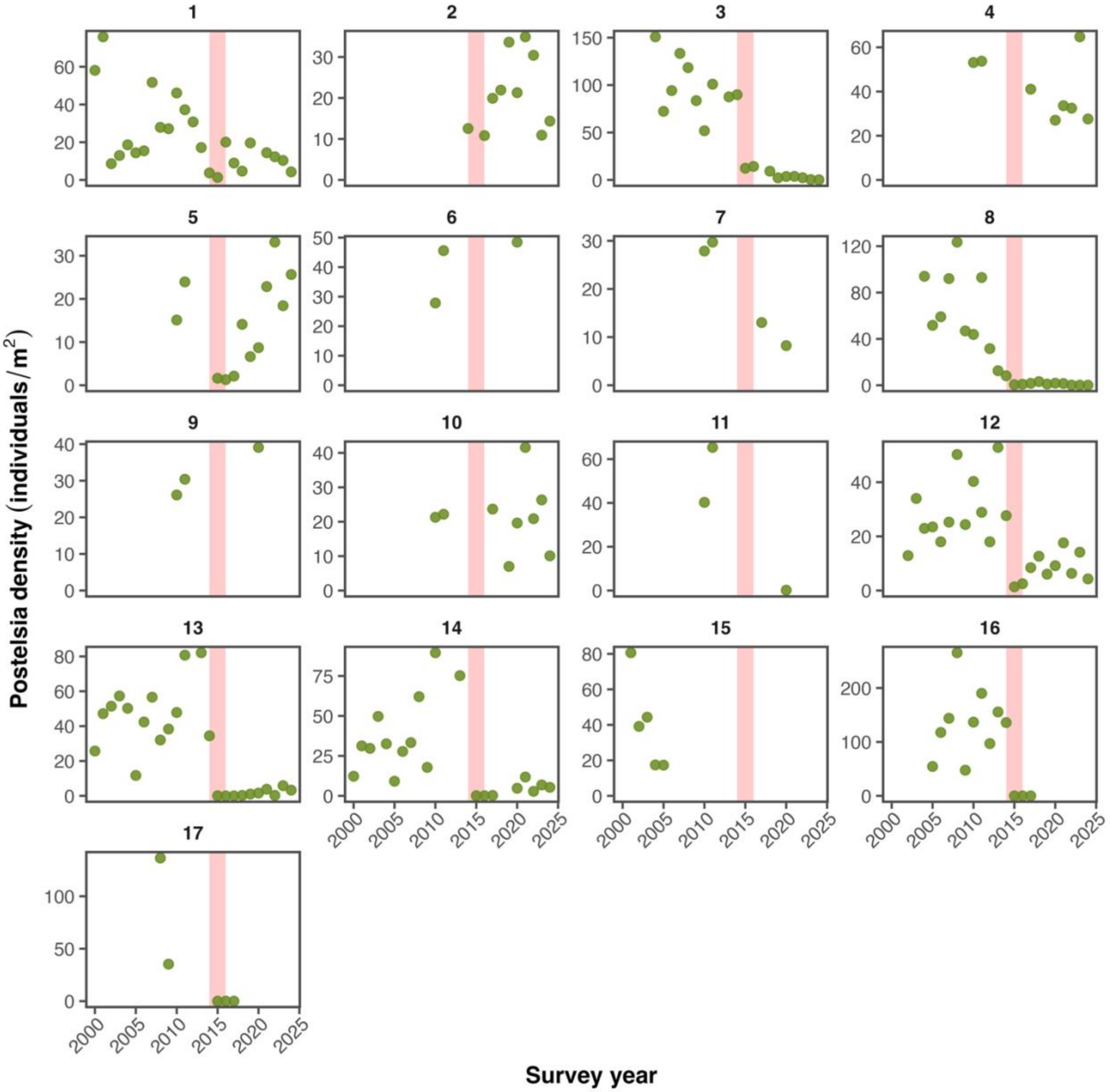

Figure S3. *Postelsia* density (# individuals/m^2) in all surveys at all sites. Shaded pink region represents the 2014-2016 MHW.

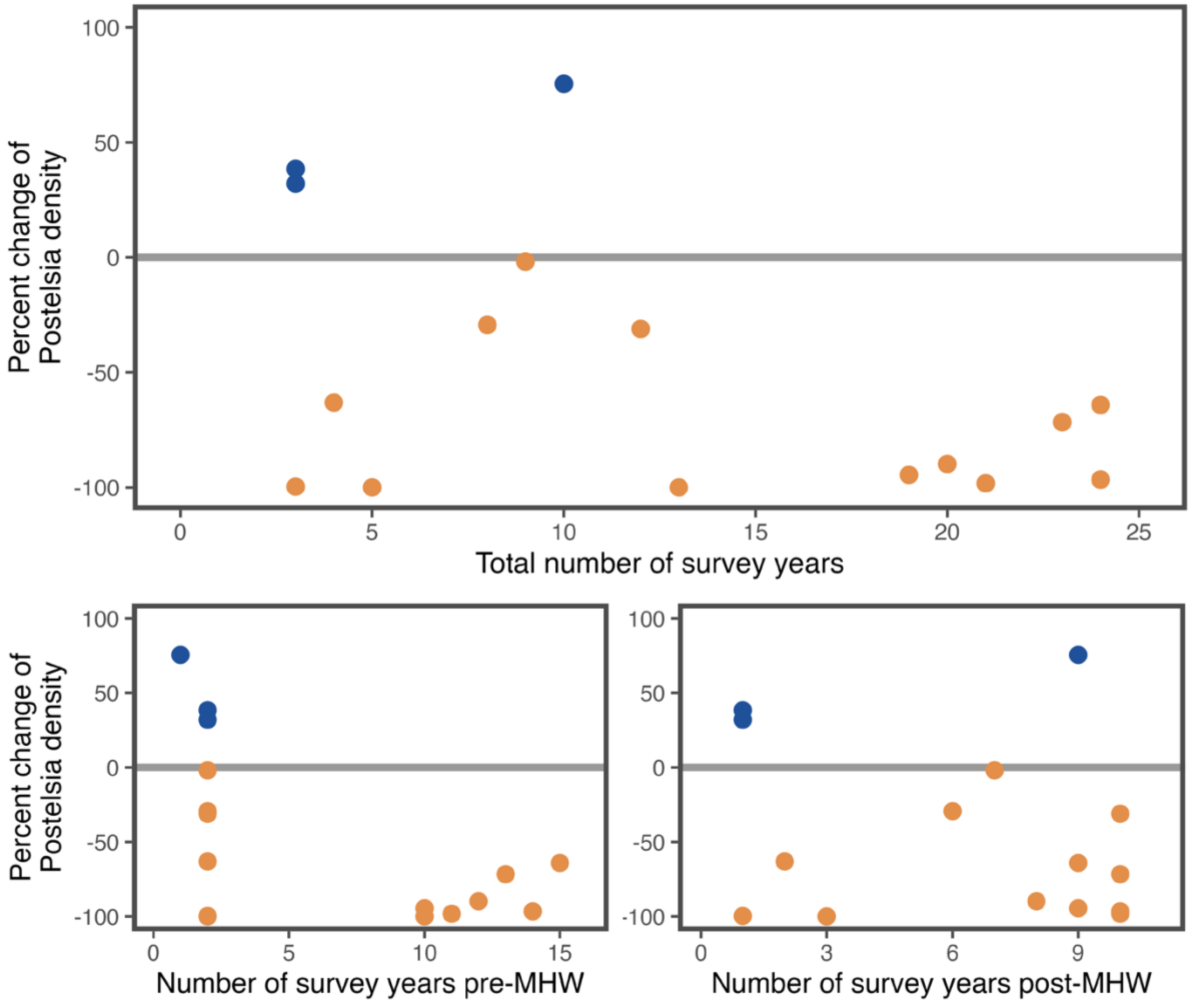

Figure S4. Percent change in mean *Postelsia* densities before (≤ 2014) versus during and after (≥ 2015) the MHW relative to **(A)** the total number of survey years, **(B)** the number of survey years pre-MHW, and **(C)** the number of survey years post-MHW (≥ 2015). Orange points indicate post-MHW declines in *Postelsia* density and blue points indicate post-MHW density increases.

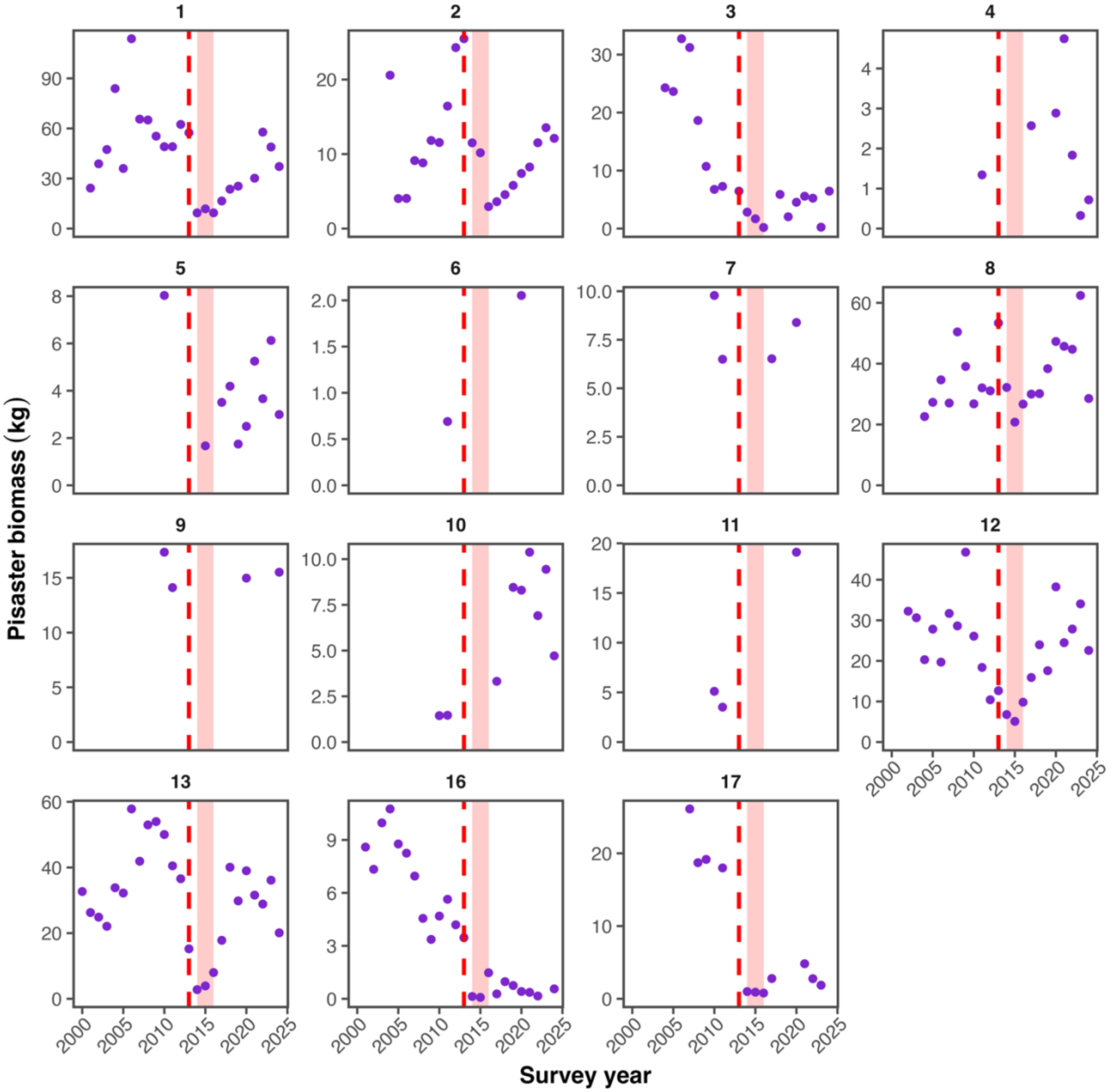

Figure S5. *Pisaster* biomass (kg) from sea star monitoring plots in all surveys at all sites. The vertical red dashed line represents the onset of the SSWD outbreak and the shaded pink region represents the 2014-2016 MHW. Note that survey area differed between sites, and we purposefully did not calculate *Pisaster* densities due to differences in habitat availability and intertidal features between sites.

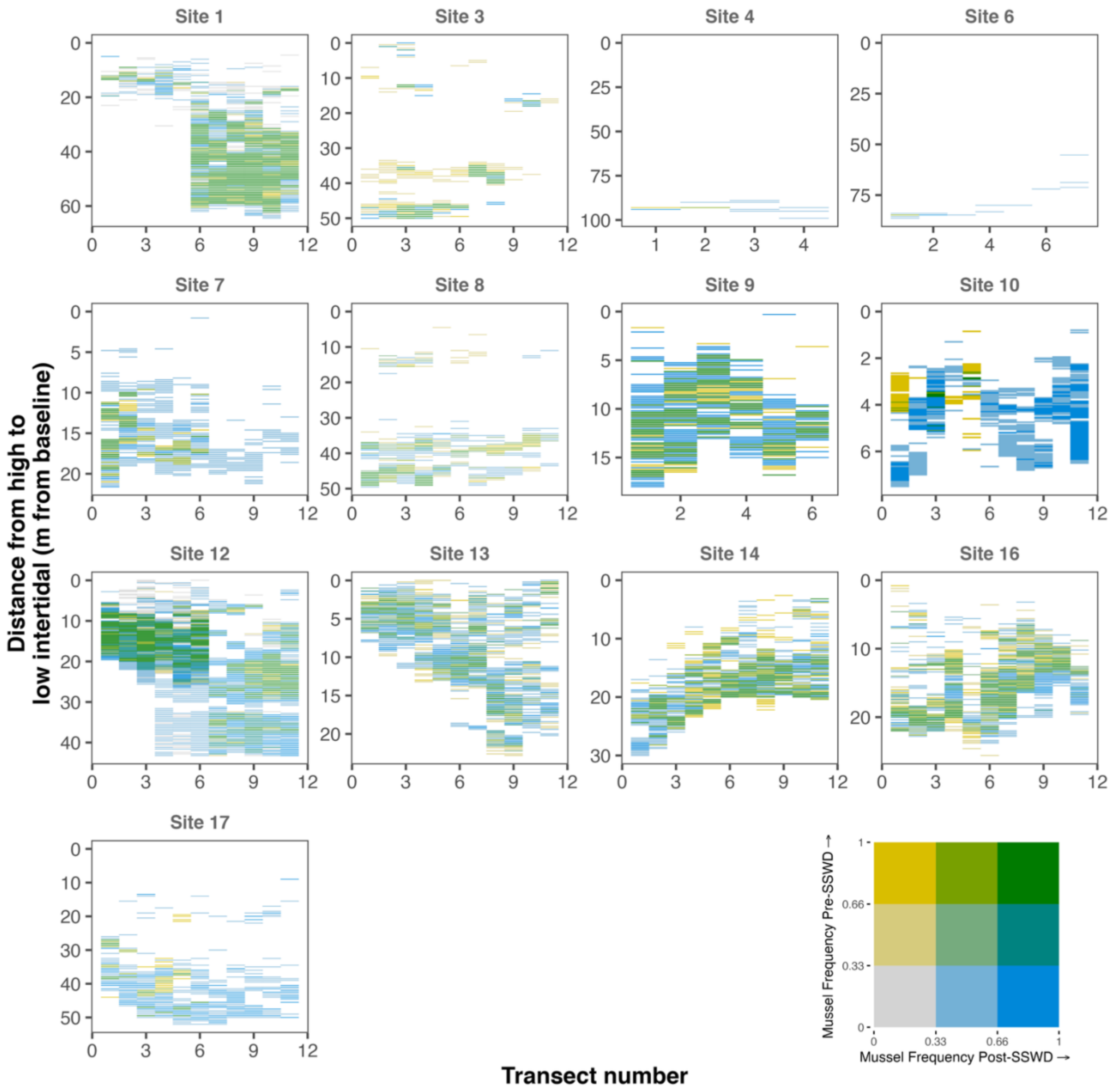

Figure S6. Presence of mussels (*M. californianus*) at replicate CBS transects (x axis) along a high-to-low (y axis) rocky intertidal gradient. Bands are colored using a bivariate palette showing mussel occurrence frequency (proportion of surveys in which mussels were detected at any single CBS survey point) before (≤ 2014; yellow scale) and after (blue scale) the SSWD outbreak. Yellow bands indicate high pre-SSWD and low post-SSWD mussel occurrence, blue bands indicate low pre-SSWD and high post-SSWD occurrence, and green bands indicate high occurrence both before and after. Uncolored points represent locations where mussels were never detected.

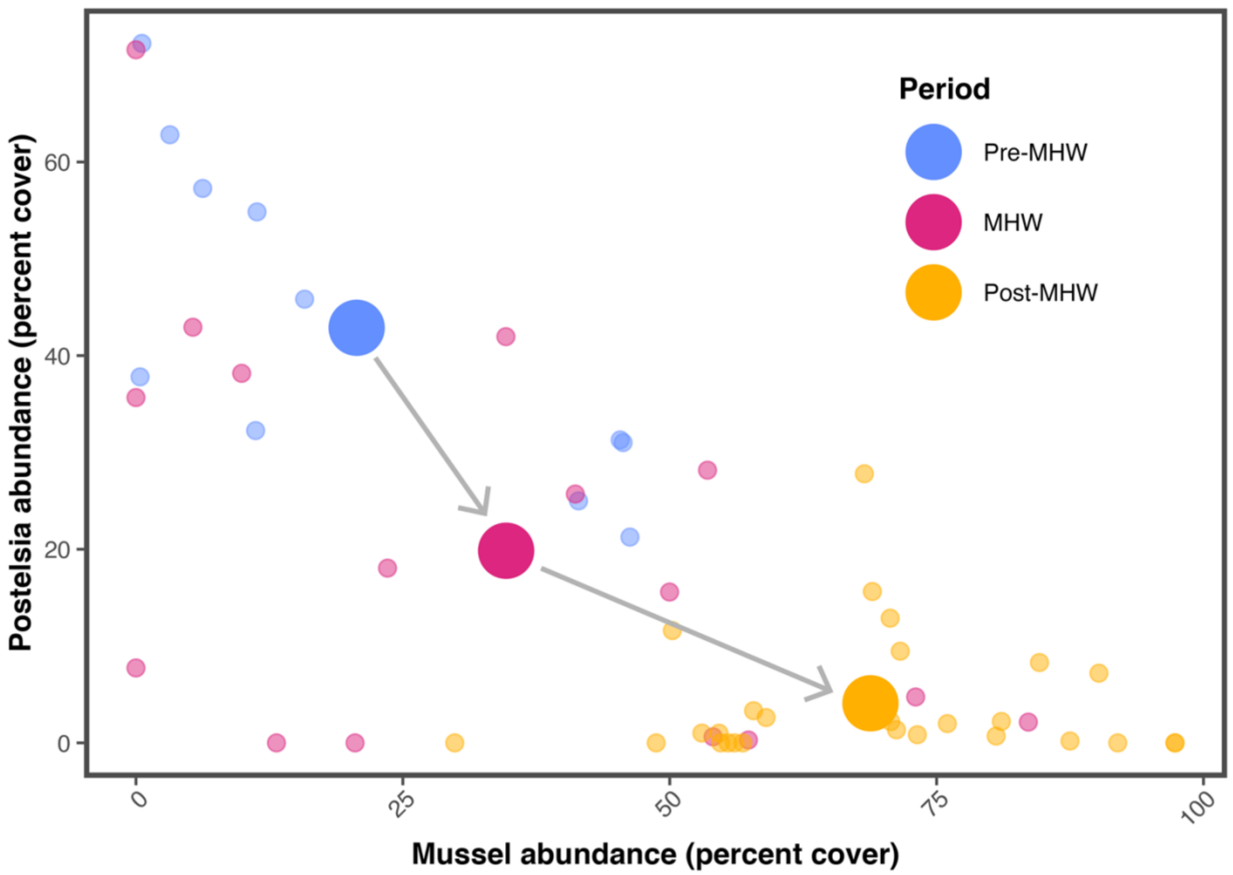

Figure S7. Temporal changes in the percent cover of *Postelsia* and mussels (*M. californianus*) within standardized boxes in repeated panoramic photos across three periods: Pre-MHW (≤ 2013), MHW (2014-2016), and Post-MHW (≥ 2017). Small points represent individual photos; large points show mean values for each period.

Table S1. Site-level summarization of rocky intertidal water temperature data.

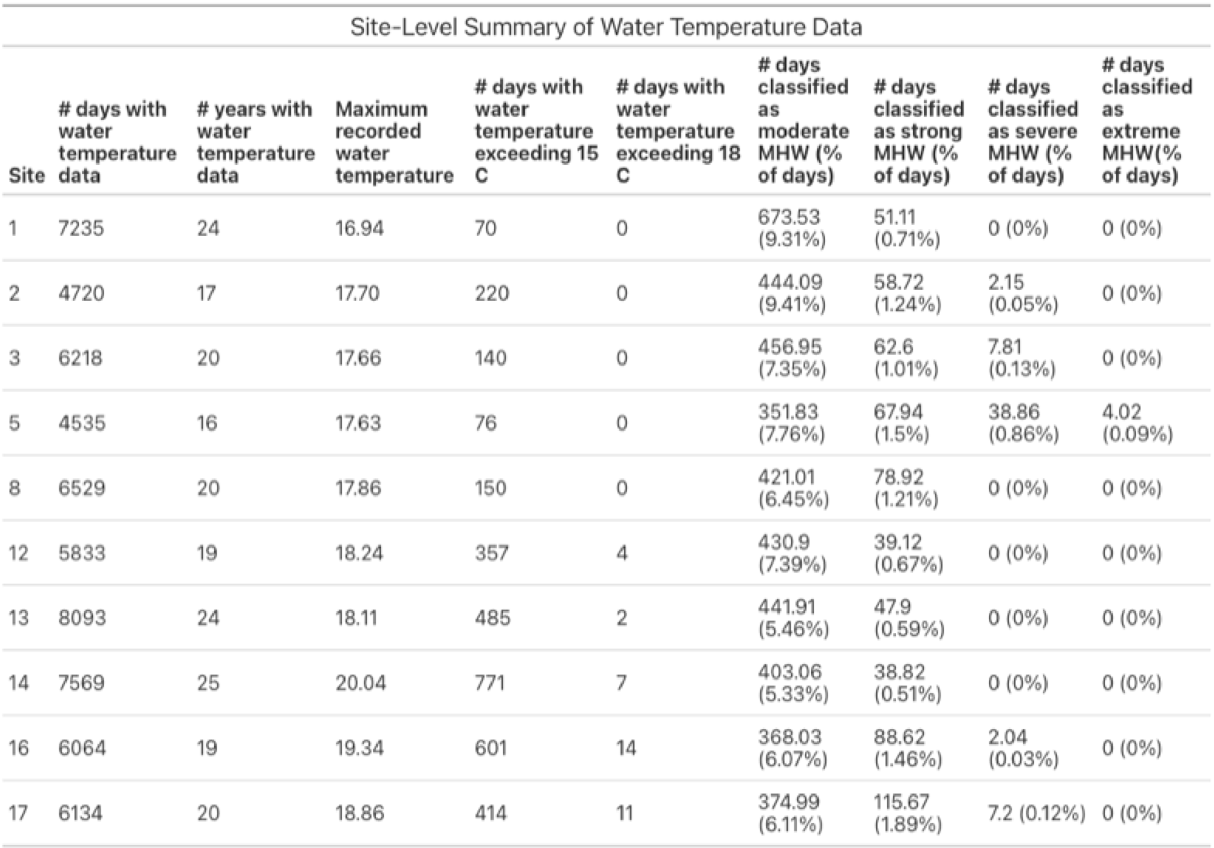

Site-Level Summary of Water Temperature Data

Site	# days with water temperature data	# years with water temperature data	Maximum recorded water temperature	# days with water temperature exceeding 15 C	# days with water temperature exceeding 18 C	# days classified as moderate MHW (% of days)	# days classified as strong MHW (% of days)	# days classified as severe MHW (% of days)	# days classified as extreme MHW(% of days)
1	7235	24	16.94	70	0	673.53 (9.31%)	51.11 (0.71%)	0 (0%)	0 (0%)
2	4720	17	17.70	220	0	444.09 (9.41%)	58.72 (1.24%)	2.15 (0.05%)	0 (0%)
3	6218	20	17.66	140	0	456.95 (7.35%)	62.6 (1.01%)	7.81 (0.13%)	0 (0%)
5	4535	16	17.63	76	0	351.83 (7.76%)	67.94 (1.5%)	38.86 (0.86%)	4.02 (0.09%)
8	6529	20	17.86	150	0	421.01 (6.45%)	78.92 (1.21%)	0 (0%)	0 (0%)
12	5833	19	18.24	357	4	430.9 (7.39%)	39.12 (0.67%)	0 (0%)	0 (0%)
13	8093	24	18.11	485	2	441.91 (5.46%)	47.9 (0.59%)	0 (0%)	0 (0%)
14	7569	25	20.04	771	7	403.06 (5.33%)	38.82 (0.51%)	0 (0%)	0 (0%)
16	6064	19	19.34	601	14	368.03 (6.07%)	88.62 (1.46%)	2.04 (0.03%)	0 (0%)
17	6134	20	18.86	414	11	374.99 (6.11%)	115.67 (1.89%)	7.2 (0.12%)	0 (0%)

Table S2. *Postelsia* density change at each site before (≤ 2014) versus during and after (≥ 2015) the MHW.

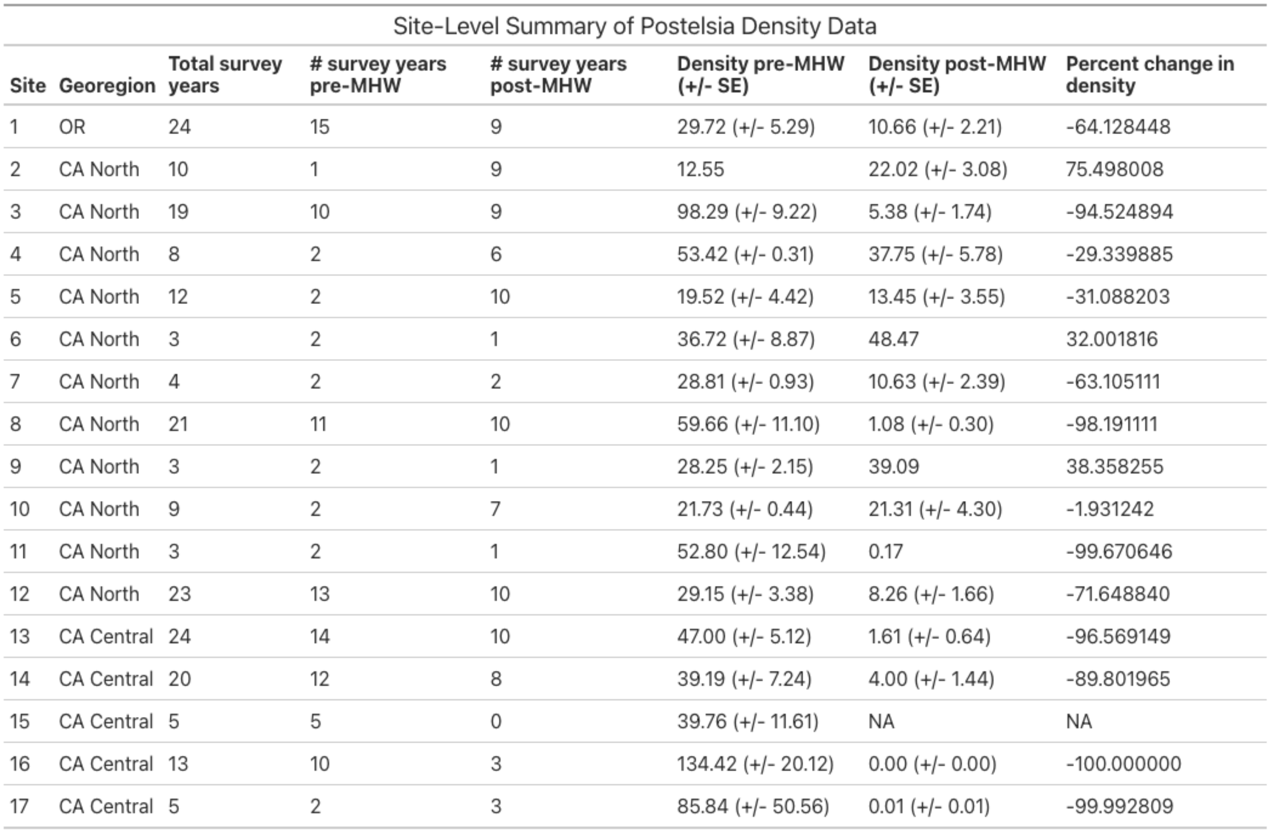

Site-Level Summary of Postelsia Density Data

Site	Georegion	Total survey years	# survey years pre-MHW	# survey years post-MHW	Density pre-MHW (+/- SE)	Density post-MHW (+/- SE)	Percent change in density
1	OR	24	15	9	29.72 (+/- 5.29)	10.66 (+/- 2.21)	-64.128448
2	CA North	10	1	9	12.55	22.02 (+/- 3.08)	75.498008
3	CA North	19	10	9	98.29 (+/- 9.22)	5.38 (+/- 1.74)	-94.524894
4	CA North	8	2	6	53.42 (+/- 0.31)	37.75 (+/- 5.78)	-29.339885
5	CA North	12	2	10	19.52 (+/- 4.42)	13.45 (+/- 3.55)	-31.088203
6	CA North	3	2	1	36.72 (+/- 8.87)	48.47	32.001816
7	CA North	4	2	2	28.81 (+/- 0.93)	10.63 (+/- 2.39)	-63.105111
8	CA North	21	11	10	59.66 (+/- 11.10)	1.08 (+/- 0.30)	-98.191111
9	CA North	3	2	1	28.25 (+/- 2.15)	39.09	38.358255
10	CA North	9	2	7	21.73 (+/- 0.44)	21.31 (+/- 4.30)	-1.931242
11	CA North	3	2	1	52.80 (+/- 12.54)	0.17	-99.670646
12	CA North	23	13	10	29.15 (+/- 3.38)	8.26 (+/- 1.66)	-71.648840
13	CA Central	24	14	10	47.00 (+/- 5.12)	1.61 (+/- 0.64)	-96.569149
14	CA Central	20	12	8	39.19 (+/- 7.24)	4.00 (+/- 1.44)	-89.801965
15	CA Central	5	5	0	39.76 (+/- 11.61)	NA	NA
16	CA Central	13	10	3	134.42 (+/- 20.12)	0.00 (+/- 0.00)	-100.000000
17	CA Central	5	2	3	85.84 (+/- 50.56)	0.01 (+/- 0.01)	-99.992809